

Diagrammatics, Pentagon Equations, and Hexagon Equations of Topological Orders with Loop- and Membrane-like Excitations

Yizhou Huang,¹ Zhi-Feng Zhang,² and Peng Ye^{1,*}

¹*School of Physics, Sun Yat-sen University, Guangzhou, 510275, China*

²*Max Planck Institute for the Physics of Complex Systems,
Nöthnitzer Straße 38, Dresden 01187, Germany*

(Dated: Wednesday 19th February, 2025)

Abstract

In spacetime dimensions of 4 (i.e., 3+1) and higher, topological orders exhibit spatially extended excitations like loops and membranes, which support diverse topological data characterizing braiding, fusion, and shrinking processes, despite the absence of anyons. Our understanding of these topological data remains less mature compared to 3D, where anyons have been extensively studied and can be fully described through diagrammatic representations. Inspired by recent advancements in field theory descriptions of higher-dimensional topological orders, this paper systematically constructs diagrammatic representations for 4D and 5D topological orders, generalizable to higher dimensions. We introduce elementary diagrams for fusion and shrinking processes, treating them as vectors in fusion and shrinking spaces, respectively, and build complex diagrams by combining these elementary diagrams. Within these vector spaces, we design unitary operations represented by F -, Δ -, and Δ^2 -symbols to transform between different bases. We discover *pentagon equations* and (*hierarchical*) *shrinking-fusion hexagon equations* that impose constraints on the legitimate forms of these unitary operations. We conjecture that all anomaly-free higher-dimensional topological orders must satisfy these conditions and any violations indicate a quantum anomaly. This work opens promising avenues for future research, including the exploration of diagrammatic representations involving braiding and the study of non-invertible symmetries and symmetry topological field theories in higher spacetime dimensions.

* Corresponding author; yepeng5@mail.sysu.edu.cn

CONTENTS

I. Introduction	3
II. Path-integral formalism of topological data	7
A. BF theory with twisted terms	7
B. Wilson operators for topological excitations	9
C. Fusion and shrinking rules in path integral formalism	11
III. Fusion and shrinking rules as mappings	16
A. 4D topological orders	16
B. 5D topological orders	18
IV. Diagrammatics of 4D topological orders	21
A. Fusion diagrams: fusion space, F -symbols, and pentagon relation	21
B. Shrinking diagrams: shrinking space and Δ -symbol	24
C. Shrinking-fusion hexagon equation	28
V. Diagrammatics of 5D topological orders	30
A. Fusion diagrams	30
B. Hierarchical shrinking diagrams and Δ^2 -symbols	31
C. Diagrammatics of the hierarchical shrinking-fusion hexagon equation	34
VI. Summary and outlook	36
Acknowledgments	38
A. Review of anyon diagrams	38
1. Fusion rules and diagrammatic representations	38
2. Braiding statistics and diagrammatic representations	41
B. Diagrams involving four excitations	42
References	45

I. INTRODUCTION

The concept of topological order was introduced in condensed matter physics to describe exotic phases of matter characterized by long-range entanglement [1]. Going beyond traditional symmetry-breaking theory, topological order has captured significant interest across various fields, including condensed matter physics, high-energy physics, mathematical physics, and quantum information [2]. Literature has explored diverse properties of topological orders, encompassing the existence of topological excitations, fusion rules, braiding statistics, and chiral central charge, collectively constituting the “topological data” crucial for their characterization and classification. One method of acquiring these data is through the path-integral formalism of topological quantum field theory (TQFT) [3, 4]. A notable example of TQFT is the 3D¹ Chern-Simons theory [5–7], which describes the low-energy, long-wavelength physics of 3D topological orders (known as anyon models) like fractional quantum Hall states. As a side note, the Chern-Simons theory is also applied to describe 3D symmetry-protected topological phases (SPT) and symmetry enriched topological phases (SET) by implementing global symmetry transformations, see, e.g., Refs. [8–11]. Anyon properties, such as fusion rules and braiding statistics, can be systematically computed within the field-theoretical framework. Moreover, fusion and braiding can be depicted diagrammatically, with the corresponding diagrammatic algebra closely linked to TQFT and topological quantum computation [12–21]. Within anyon diagrams, F -symbols and R -symbols can be defined to facilitate transformations between different diagrams, subject to consistency conditions like the pentagon and hexagon equations in anomaly-free topological orders².

Topological orders in 3D have been extensively explored through the lenses of TQFT and category theory. How about higher-dimensional topological orders? In 4D, topological excitations include both point-like particles and one-dimensional loop excitations, hereafter referred to as “particles” and “loops” for brevity. While mutual braidings among particles are trivial in 4D and higher dimensions [22–27], the presence of topological excitations with spatially extended shapes significantly expands the potential for braiding and fusion properties. Moreover, the existence of spatially extended shapes allows for the consideration of shrinking rules [28, 29], which dictate how loops can be shrunk into particles across one or more channels. Notably, nontrivial shrinking

¹ Unless otherwise specified, 3D, 4D, and 5D always represent dimensions of spacetime. That is, 3D=(2+1)D, 4D=(3+1)D, and 5D=(4+1)D.

² For more details about anyon diagrams, we recommend the relevant section in the research article [21] as well as the book [19]. Appendix A is also supplemented for an introduction to pentagon equations and braiding-fusion hexagon equations in anyon models.

rules can only manifest in topological orders in 4D and higher, where topological excitations with spatially extended shapes exist. In 3D, a loop excitation is topologically indistinguishable from anyons since the braiding process is unable to detect the geometric hole of the loop excitation.

Analogous to the Chern-Simons field theory description of 3D topological orders, when particles and loops in 4D are respectively represented by charges and fluxes of an Abelian finite gauge group, the BF theory and its twisted variants [30–41] have been applied to describe 4D topological orders as well as *gauged* SPTs, which also attract a lot of investigations from non-invertible symmetry and symmetry topological field theory (SymTFT) [42–55]. The BF term (BdA in which B and A are respectively 2- and 1-form gauge fields) equipped with various twisted terms (e.g., $AAAdA$, $AAAA$, AAB , $dAdA$, and BB) enables systematic computation of topological data, such as particle-loop braiding [24, 25, 56–58], multi-loop braiding [34, 59–68], particle-loop-loop braiding (i.e., Borromean rings braiding) [38], emergent fermionic statistics [35, 40, 69, 70], and topological response [31, 33, 41, 71–75]. Refs. [76–78] field-theoretically demonstrate how global symmetry is fractionalized on loop excitations. There, the concept of “mixed three-loop braiding” processes is introduced, leading to a classification scheme of SETs in higher dimensions. Importantly, braiding data discovered above are not always allowed to coexist. It has been shown that there exists important compatibility among these braiding processes [39], ruling out gauge-non-invariant combinations of braiding processes. Furthermore, loop excitations in Borromean rings topological order [38] can exhibit non-Abelian fusion and shrinking rules [28], despite the gauge charges carried by loops being Abelian. At the same time, all shrinking rules are consistent with fusion rules in the sense that fusion coefficients and shrinking coefficients together should satisfy consistency conditions [28]. On the other hand, the emergence of fermions is also a fundamental issue. By studying correlation functions of Wilson operators equipped with the framing regularization, Ref. [70] investigates how fermionic statistics of particle excitations can emerge in the low-energy gauge theory, successfully incorporating the data of self-statistics of particle excitations.

When considering topological orders in 5D, the topological data become even more exotic. Topological excitations now include particles, loops, and two-dimensional membranes, highlighting unexplored features of topological orders. From a field-theoretical perspective, we can still employ BF field theory to investigate braiding statistics, fusion rules, and shrinking rules. The BF term can take the form of either CdA or $\tilde{B}dB$, where C represents 3-form gauge fields, \tilde{B} and B represent different 2-form gauge fields. These terms can be further enriched with various

twisted terms, such as $AAAAA$, $AAAdA$, $AdAdA$, AAC , $AAAB$, BBA , $AdAB$, $AAdB$, and BC [79]. Recently, several exotic braiding processes have been computed via these 5D topological terms [79], resulting in mathematically nontrivial links formed by closed spacetime trajectories of particles, loops, and membranes. Technically, braiding statistics can be systematically computed by evaluating correlation functions of Wilson operators, whose expectation values are related to intersections of sub-manifolds embedded in the 5D spacetime manifold. Additionally, exotic fusion and shrinking rules in 5D have been explored [29]. Some membranes exhibit hierarchical shrinking rules, where a membrane shrinks into particles and loops, followed by the subsequent shrinking of loops into particles. Such nontrivial *hierarchical shrinking* structures can only exist in 5D and higher.

We have mentioned that the topological data of anyon models in 3D can be schematically represented by diagrams, with their corresponding algebraic structure related to TQFT and category theory. Using diagrammatic representations is beneficial for understanding the universal properties of topological orders and their underlying mathematical structures, which plays a critical role in unitary operations for realizing topological quantum computation [19]. Important consistency conditions, such as the celebrated *pentagon and hexagon equations* can be efficiently handled via diagrams. However, there is still a lack of research on diagrammatic representations of higher-dimensional topological orders, which hinders a systematic exploration of topologically ordered phases in higher dimensions. Especially, the presence of loop excitations and membrane excitations is expected to significantly enrich the potential constraints beyond 3D anyon theory. Inspired by the aforementioned progress in field theory in 4D and 5D, in this work, we aim to construct diagrammatic representations capable of describing the exotic properties of higher-dimensional topological orders in this paper.

In our diagrammatic representations, excitations are categorized into different sets, and we use different types of straight lines (e.g., single-line, double-line) to represent them. Given that fusion rules still satisfy the associativity condition, we can define fusion diagrams and F -symbols, similar to the case in 3D. Changing the order of fusion processes in a diagram is implemented by F -symbols, which can be understood as basis transformations. To describe (hierarchical) shrinking processes and the consistent relation between (hierarchical) shrinking and fusion, we define (hierarchical) shrinking diagrams and Δ -symbols (Δ^2 -symbols). Changing the order of fusion and (hierarchical) shrinking processes in a diagram is implemented by such Δ -symbols (Δ^2 -symbols), which can also be viewed as basis transformations. Having defined F -symbols and Δ -symbols

(Δ^2 -symbols), we further discover a series of equations that must be implemented for these symbols. First, F -symbols still satisfy the “*pentagon equation*”; second, F -symbols and Δ -symbols (Δ^2 -symbols) jointly satisfy the so-called “*(hierarchical) shrinking-fusion hexagon equations*”. We conjecture that all anomaly-free topological orders in higher-dimensional spacetime should satisfy these equations. A quantum anomaly appears if one of these equations is not satisfied. It should be noted that the diagrams we construct in this paper involve fusion and (hierarchical) shrinking processes, thereby reflecting the algebraic structure of consistent fusion and (hierarchical) shrinking rules. As for braiding processes, since they may involve more than two excitations and thus form various kinds of exotic links, the diagrammatic representations may be considerably more complicated, and we leave them for future exploration.

This paper is organized as follows. In section II, we first review some basic concepts and properties of fusion and (hierarchical) shrinking rules, with a particular focus on their path-integral formalism established in our previous studies. We conclude that fusion rules respect (hierarchical) shrinking rules, which lays the foundation for our construction of diagrammatic representations of fusion and (hierarchical) shrinking rules. In section III, we study fusion and shrinking in 4D and 5D as mappings between different sets of excitations. Since excitations from different sets play distinct roles in (hierarchical) shrinking processes, we need to treat them differently in our diagrams. In section IV, we focus on 4D topological orders. Based on what we have established in section III and IV, we define basic fusion and shrinking diagrams and combine them to generate more complex diagrams. By introducing F - and Δ -symbols, we can transform diagrams and ultimately obtain the pentagon equation and (hierarchical) shrinking-fusion hexagon equation, which are key equations in our diagrammatic representations. In section V, we extend our construction to 5D topological orders, introducing hierarchical shrinking diagrams and unitary operations denoted as Δ^2 -symbols. Following a similar strategy, we derive a new consistency relation called the “*hierarchical shrinking-fusion hexagon equation*”. A brief summary is provided in section VI, in which several promising future directions are discussed. Two appendices are supplemented. In appendix A, we offer a short review of diagrammatic representations of 3D topological orders (anyon models). Appendix B discusses the completeness of pentagon equations and shrinking-fusion hexagon equations.

II. PATH-INTEGRAL FORMALISM OF TOPOLOGICAL DATA

In this section, we will review several field-theoretical results established before [28, 29], where path-integral formalism is applied. We first present two typical twisted terms in BF theory, both of which can lead to non-Abelian fusion rules and nontrivial (hierarchical) shrinking rules. Then we give several examples of constructing gauge invariant Wilson operators for topological excitations. Meanwhile, we will explain the meaning of several useful notations that were introduced in our previous papers [28, 29], which will be frequently used in establishing the notion of “set of excitations” in section III. Finally, we elaborate on how to calculate fusion and (hierarchical) shrinking rules in path-integral formalism. By exhausting all possible fusion and (hierarchical) shrinking processes, we conclude that in 4D BF theory, fusion rules respect shrinking rules, i.e. satisfy eq. (20). While in 5D, there exist nontrivial hierarchical shrinking rules. Fusion rules no longer respect shrinking rules in 5D generally. Instead, fusion rules respect hierarchical shrinking rules, i.e., satisfy eq. (21). The two relations (20) and (21) are the key results in our previous works [28, 29]. Our construction of diagrammatic representations is essentially based on these two relations.

A. BF theory with twisted terms

We consider BF theory as the underlying TQFT for higher-dimensional topological orders. The topological action consists of BF terms and twisted terms. The BF term BdA ³ in 4D is written as a wedge product of B and dA , where B and A are respectively 2- and 1-form gauge fields. Twisted terms in 4D consist of $AAAdA$, $AAAA$, AAB , $dAdA$ and BB terms. While in 5D, BF terms include CdA and $\tilde{B}dB$ terms, where C is 3-form, B and \tilde{B} are two different 2-form, A is 1-form. Twisted terms now include $AAAAA$, $AAAdA$, $AdAdA$, AAC , $AAAB$, BBA , $AdAB$, $AAdB$ and BC terms. A BF action can contain several different twisted terms as long as the action is gauge invariant [39, 70].

To better illustrate fusion and shrinking rules from TQFT, below we introduce two typical BF actions first [28, 29]. For simplicity, we only consider one twisted term and take the discrete Abelian gauge group as $G = \prod_{i=1}^n \mathbb{Z}_{N_i} = (\mathbb{Z}_2)^3$. In 4D, we choose the twisted term to be the

³ The wedge product “ \wedge ” is omitted for the notational convenience.

AAB term and write the action as:

$$S = \int \frac{N_1}{2\pi} B^1 dA^1 + \frac{N_2}{2\pi} B^2 dA^2 + \frac{N_3}{2\pi} B^3 dA^3 + q A^1 A^2 B^3, \quad (1)$$

where A^i and B^i are 1- and 2-form gauge fields respectively. The coefficient $q = \frac{pN_1N_2N_3}{(2\pi)^2N_{123}}$, where $p \in \mathbb{Z}_{N_{123}}$ and N_{123} is the greatest common divisor of N_1 , N_2 , and N_3 . A^1 , A^2 and B^3 satisfy the flat-connection conditions: $dA^1 = 0$, $dA^2 = 0$, and $dB^3 = 0$. The gauge transformations are:

$$\begin{aligned} A^1 &\rightarrow A^1 + d\chi^1, & A^2 &\rightarrow A^2 + d\chi^2, & B^3 &\rightarrow B^3 + dV^3, \\ B^1 &\rightarrow B^1 + dV^1 - \frac{2\pi q}{N_1} (\chi^2 B^3 - A^2 V^3 + \chi^2 dV^3), \\ B^2 &\rightarrow B^2 + dV^2 + \frac{2\pi q}{N_2} (\chi^1 B^3 - A^1 V^3 + \chi^1 dV^3), \\ A^3 &\rightarrow A^3 + d\chi^3 - \frac{2\pi q}{N_3} \left(\chi^1 A^2 - \chi^2 A^1 + \frac{1}{2} \chi^1 d\chi^2 - \frac{1}{2} \chi^2 d\chi^1 \right), \end{aligned} \quad (2)$$

where χ^i and V^i are 0-form and 1-form gauge parameters respectively. They satisfy the following compactness conditions: $\int d\chi^i \in 2\pi\mathbb{Z}$ and $\int dV^i \in 2\pi\mathbb{Z}$. Another example is the action that contains the BBA twisted term in 5D, we still consider $G = \prod_{i=1}^n \mathbb{Z}_{N_i} = (\mathbb{Z}_2)^3$ and write the action as:

$$S = \int \frac{N_1}{2\pi} \tilde{B}^1 dB^1 + \frac{N_2}{2\pi} \tilde{B}^2 dB^2 + \frac{N_3}{2\pi} C^3 dA^3 + q B^1 B^2 A^3, \quad (3)$$

where A^3 , B^i , \tilde{B}^i , and C^3 are 1-, 2-, 2-, and 3-form gauge fields respectively. The coefficient $q = \frac{pN_1N_2N_3}{(2\pi)^2N_{123}}$, where $p \in \mathbb{Z}_{N_{123}}$ and N_{123} is the greatest common divisor of N_1 , N_2 and N_3 . The flat-connection conditions are $dB^1 = 0$, $dB^2 = 0$, and $dA^3 = 0$. The gauge transformations are given by:

$$\begin{aligned} B^1 &\rightarrow B^1 + dV^1, & B^2 &\rightarrow B^2 + dV^2, & A^3 &\rightarrow A^3 + d\chi^3, \\ \tilde{B}^1 &\rightarrow \tilde{B}^1 + d\tilde{V}^1 + \frac{2\pi q}{N_1} (V^2 A^3 + B^2 \chi^3 + V^2 d\chi^3), \\ \tilde{B}^2 &\rightarrow \tilde{B}^2 + d\tilde{V}^2 + \frac{2\pi q}{N_2} (V^1 A^3 + B^1 \chi^3 + V^1 d\chi^3), \\ C^3 &\rightarrow C^3 + dT^3 - \frac{2\pi q}{N_3} \left(V^1 B^2 + B^1 V^2 + \frac{1}{2} V^1 dV^2 + \frac{1}{2} V^2 dV^1 \right), \end{aligned} \quad (4)$$

where χ^3 , V^i , \tilde{V}^i and T^3 are 0-, 1-, 1- and 2-form gauge parameters respectively. The compactness conditions are: $\int d\chi^3 \in 2\pi\mathbb{Z}$, $\int dV^i \in 2\pi\mathbb{Z}$, $\int d\tilde{V}^i \in 2\pi\mathbb{Z}$, and $\int dT^3 \in 2\pi\mathbb{Z}$. The two examples above both have non-Abelian fusion and shrinking rules. Besides, the BBA twisted term also admits hierarchical shrinking rules.

B. Wilson operators for topological excitations

In TQFT, topological excitations carry gauge charges minimally coupled to gauge fields. Thus, by respectively using gauge fields of 1-, 2-, and 3-form, we can construct Wilson loop operators for particle excitations, Wilson surface operators for loop excitations, and Wilson volume operators for membrane excitations. We use the Wilson operator \mathcal{O}_a to represent the topological excitation a in the path integral formalism. Following the notations in refs. [28, 29], we present some examples of these Wilson operators.

A particle can only carry gauge charges minimally coupled to 1-form gauge fields A and we generally use $P_{n_1 n_2 \dots n_k}$ to represent a particle simultaneously carrying n_1, n_2, \dots, n_k units of $\mathbb{Z}_{N_1}, \mathbb{Z}_{N_2}, \dots, \mathbb{Z}_{N_k}$ gauge charge. The Wilson operator for such excitation should be constructed by using k gauge fields A^1, A^2, \dots, A^k . Consider BBA twisted terms as an example, a particle carrying unit gauge charge minimally coupled to 1-form gauge field A^3 is denoted as P_{001} , which can be represented by the following gauge invariant Wilson operator $\mathcal{O}_{P_{001}}$:

$$\mathcal{O}_{P_{001}} = \exp \left(i \int_{\gamma} A^3 \right), \quad (5)$$

where $\gamma = S^1$ is the closed world-line of the particle. Since the action (3) contains only one 1-form gauge field, i.e., A^3 , only n_3 can be nonzero. Since $G = (\mathbb{Z}_2)^3$, n_3 only takes 0 or 1 mod 2 here.

A loop in 5D can carry gauge charges minimally coupled to 2-form gauge fields and be decorated by particles, i.e., the loop can be decorated by gauge charges minimally coupled to 1-form gauge fields. We generally use $L_{n_1 n_2 \dots n_k, \tilde{n}_1 \tilde{n}_2 \dots \tilde{n}_k}^{m_1 m_2 \dots m_l}$ to represent a loop. Here n_1, n_2, \dots, n_k in the subscript denote n_1, n_2, \dots, n_k units of $\mathbb{Z}_{N_1}, \mathbb{Z}_{N_2}, \dots, \mathbb{Z}_{N_k}$ gauge charge minimally coupled to B^1, B^2, \dots, B^k fields respectively. $\tilde{n}_1, \tilde{n}_2, \dots, \tilde{n}_k$ in the subscript denote $\tilde{n}_1, \tilde{n}_2, \dots, \tilde{n}_k$ units of $\mathbb{Z}_{N_1}, \mathbb{Z}_{N_2}, \dots, \mathbb{Z}_{N_k}$ gauge charge minimally coupled to $\tilde{B}^1, \tilde{B}^2, \dots, \tilde{B}^k$ fields respectively. m_1, m_2, \dots, m_l in the superscript denote m_1, m_2, \dots, m_l units of $\mathbb{Z}_{N_1}, \mathbb{Z}_{N_2}, \dots, \mathbb{Z}_{N_l}$ gauge charge minimally coupled to A^1, A^2, \dots, A^l fields respectively. In BBA twisted term, a loop simultaneously carrying gauge charges minimally coupled to B^1 and B^2 and decorated by gauge charge minimally coupled to A^3 is denoted as $L_{110,000}^{001}$. The gauge invariant Wilson operator is given by

$$\mathcal{O}_{L_{110,000}^{001}} = \exp \left(i \int_{\sigma} B^1 + i \int_{\sigma} B^2 + i \int_{\gamma} A^3 \right), \quad (6)$$

where $\sigma = S^1 \times S^1 = T^2$ is the closed world sheet of the loop excitation. γ is an arbitrary closed line on σ , i.e., $\gamma \in \sigma$. For the notational simplicity, we omit 000 in the superscript and subscript,

thus $L_{110,000}^{001}$ can be rewritten as L_{110}^{001} . Note that the comma in the subscript should not be omitted. The numbers on the left side of the comma correspond to the B fields while the numbers on the right side of the comma correspond to the \tilde{B} fields.

As for membranes, we consider two different shapes: the membrane denoted by M^S is in the shape of S^2 and the membrane denoted by M^T is in the shape of T^2 . Both of them can carry gauge charges minimally coupled to 3-form fields and they can be decorated by loops and particles. The loop and particle decorations on the membrane carry gauge charges minimally coupled to 2-form and 1-form fields respectively. We generally use $M_{n_1 n_2 \dots n_k}^{S p_1 p_2 \dots p_k; m_1 m_2 \dots m_l, \tilde{m}_1 \tilde{m}_2 \dots \tilde{m}_l}$ or $M_{n_1 n_2 \dots n_k}^{T p_1 p_2 \dots p_k; m_1 m_2 \dots m_l, \tilde{m}_1 \tilde{m}_2 \dots \tilde{m}_l}$ to represent them. Here n_1, n_2, \dots, n_k in the subscript denote n_1, n_2, \dots, n_k units of $\mathbb{Z}_{N_1}, \mathbb{Z}_{N_2}, \dots, \mathbb{Z}_{N_k}$ gauge charge minimally coupled to C^1, C^2, \dots, C^k fields respectively. p_1, p_2, \dots, p_k in the superscript denote p_1, p_2, \dots, p_k units of $\mathbb{Z}_{N_1}, \mathbb{Z}_{N_2}, \dots, \mathbb{Z}_{N_k}$ gauge charge minimally coupled to A^1, A^2, \dots, A^k fields respectively. m_1, m_2, \dots, m_l in the superscript denote m_1, m_2, \dots, m_l units of $\mathbb{Z}_{N_1}, \mathbb{Z}_{N_2}, \dots, \mathbb{Z}_{N_l}$ gauge charge minimally coupled to B^1, B^2, \dots, B^l fields respectively. $\tilde{m}_1, \tilde{m}_2, \dots, \tilde{m}_l$ in the superscript denote $\tilde{m}_1, \tilde{m}_2, \dots, \tilde{m}_l$ units of $\mathbb{Z}_{N_1}, \mathbb{Z}_{N_2}, \dots, \mathbb{Z}_{N_l}$ gauge charge minimally coupled to $\tilde{B}^1, \tilde{B}^2, \dots, \tilde{B}^l$ fields respectively. For simplicity, we omit the whole superscript if there is no decoration. We also write “ $p_1 p_2 \dots ; 000, 000$ ” as “ $p_1 p_2 \dots ;$ ” and “ $000; 000, \tilde{m}_1 \tilde{m}_2 \dots$ ” as “ $, \tilde{m}_1 \tilde{m}_2 \dots$ ”, respectively. In BBA twisted term, a torus-like membrane carrying unit gauge charge minimally coupled to 3-form field C^3 is denoted as M_{001}^T . The corresponding gauge invariant Wilson operator is given by

$$\mathcal{O}_{M_{001}^T} = 4 \exp \left[i \int_{\omega} C^3 + \frac{1}{2} \frac{2\pi q}{N_3} (d^{-1} B^1 B^2 + d^{-1} B^2 B^1) \right] \delta \left(\int_{\sigma} B^1 \right) \delta \left(\int_{\sigma} B^2 \right), \quad (7)$$

where $\omega = T^2 \times S^1$ is the closed world volume of the membrane excitation. The nontrivial terms $\frac{1}{2} \frac{2\pi q}{N_3} (d^{-1} B^1 B^2 + d^{-1} B^2 B^1)$ are introduced to guarantee that the Wilson operator is gauge invariant. We define $d^{-1} B^1$ and $d^{-1} B^2$ as $d^{-1} B^1 = \int_{\mathcal{A} \in \omega} B^1$ and $d^{-1} B^2 = \int_{\mathcal{A} \in \omega} B^2$, where \mathcal{A} is an open area on ω . As 1-form fields, $d^{-1} B^1$ and $d^{-1} B^2$ are well defined on ω if and only if B^1 and B^2 are exact on ω , i.e., B^1 and B^2 satisfy extra constraints: $\int_{\sigma} B^1 = 0 \bmod 2\pi$, $\int_{\sigma} B^2 = 0 \bmod 2\pi$, where σ is an arbitrary closed surface on ω . To enforce these constraints, we introduce two delta functionals in eq. (7):

$$\delta \left(\int_{\sigma} B^1 \right) = \begin{cases} 1, & \int_{\sigma} B^1 = 0 \bmod 2\pi \\ 0, & \text{else} \end{cases}, \quad \delta \left(\int_{\sigma} B^2 \right) = \begin{cases} 1, & \int_{\sigma} B^2 = 0 \bmod 2\pi \\ 0, & \text{else} \end{cases}. \quad (8)$$

We can construct other Wilson operators for excitations by using the similar approach. In our previous papers [28, 29], we have exhausted all topologically distinct Wilson operators in BF theory with AAB and BBA twisted terms respectively. We conclude that there are 19 topologically distinct excitations in BF theory with AAB twisted term and 29 topologically distinct excitations in BF theory with BBA twisted term.

C. Fusion and shrinking rules in path integral formalism

Fusion rules of topological excitations are important topological data in topological orders. If we adiabatically bring two topological excitations together spatially, the combination of the two excitations behaves like another topological excitation. Within the framework of path integral, fusing two topological excitations a and b is represented by

$$\langle a \otimes b \rangle = \frac{1}{\mathcal{Z}} \int \mathcal{D}[ABC] \exp(iS) \times (\mathcal{O}_a \times \mathcal{O}_b). \quad (9)$$

where \mathcal{Z} and S are partition function and action respectively. $\mathcal{D}[ABC]$ represents the integration over all field configurations. Refs. [28, 29] show that we can further calculate the fusion rules as

$$\begin{aligned} \langle a \otimes b \rangle &= \frac{1}{\mathcal{Z}} \int \mathcal{D}[ABC] \exp(iS) \times (\mathcal{O}_a \times \mathcal{O}_b) \\ &= \frac{1}{\mathcal{Z}} \int \mathcal{D}[ABC] \exp(iS) \times \left(\sum_c N_c^{ab} \mathcal{O}_c \right) \\ &= \langle \oplus_c N_c^{ab} c \rangle, \end{aligned} \quad (10)$$

We can simply rewrite eq. (10) as

$$a \otimes b = \oplus_c N_c^{ab} c. \quad (11)$$

a , b and c denote topological excitations and $N_c^{ab} \in \mathbb{Z}$ is fusion coefficient implying there are N_c^{ab} fusion channels to c . Summation \oplus_c exhausts all topological excitations in the system. If $N_c^{ab} = 0$, it means that such fusion channel does not exist and fusing a and b to c is prohibited. A fusion process that only has a single fusion channel is called an Abelian fusion process. In contrast, a non-Abelian fusion process contains multiple fusion channels, indicating different possible fusion outputs. For an excitation a , if fusing a and b is always Abelian for any b , we call a an Abelian excitation. Otherwise, we call a a non-Abelian excitation. Fusion rules satisfy commutativity and

associativity, i.e.,

$$\mathbf{a} \otimes \mathbf{b} = \mathbf{a} \otimes \mathbf{b}, \quad (12)$$

$$(\mathbf{a} \otimes \mathbf{b}) \otimes \mathbf{c} = \mathbf{a} \otimes (\mathbf{b} \otimes \mathbf{c}). \quad (13)$$

Following the notations in ref. [28], here we present an explicit example of fusing two loops. A loop in the AAB twisted term carrying unit gauge charge minimally coupled to B^1 is denoted as \mathbf{L}_{100} , which can be represented by [28]

$$\mathcal{O}_{\mathbf{L}_{100}} = 2 \exp \left[i \int_{\sigma} B^1 + \frac{1}{2} \frac{2\pi q}{N_1} (d^{-1} A^2 B^3 + d^{-1} B^3 A^2) \right] \delta \left(\int_{\gamma} A^2 \right) \delta \left(\int_{\sigma} B^3 \right). \quad (14)$$

We define $d^{-1} A^2$ and $d^{-1} B^3$ as $d^{-1} A^2 = \int_{[a,b] \in c} A^2$ and $d^{-1} B^3 = \int_{\mathcal{A} \in \sigma} B^3$ respectively, where $[a, b]$ is a segment of the closed curve c and \mathcal{A} is an open area on σ . The delta functionals are:

$$\begin{aligned} \delta \left(\int_{\sigma} A^2 \right) &= \begin{cases} 1, & \int_{\gamma} A^2 = 0 \pmod{2\pi} \\ 0, & \text{else} \end{cases}, \\ \delta \left(\int_{\sigma} B^3 \right) &= \begin{cases} 1, & \int_{\sigma} B^3 = 0 \pmod{2\pi} \\ 0, & \text{else} \end{cases}. \end{aligned} \quad (15)$$

Thus fusing two \mathbf{L}_{100} 's is given by:

$$\begin{aligned} &\langle \mathbf{L}_{100} \otimes \mathbf{L}_{100} \rangle \\ &= \frac{1}{\mathcal{Z}} \int \mathcal{D}[AB] \exp(iS) \times \mathcal{O}_{\mathbf{L}_{100}} \times \mathcal{O}_{\mathbf{L}_{100}} \\ &= \frac{1}{\mathcal{Z}} \int \mathcal{D}[AB] \exp(iS) \times \left\{ 2 \exp \left[i \int_{\sigma} B^1 + \frac{1}{2} \frac{2\pi q}{N_1} (d^{-1} A^2 B^3 + d^{-1} B^3 A^2) \right] \right. \\ &\quad \left. \times \delta \left(\int_{\gamma} A^2 \right) \delta \left(\int_{\sigma} B^3 \right) \right\}^2 \\ &= \frac{1}{\mathcal{Z}} \int \mathcal{D}[AB] \exp(iS) \times \left[1 + \exp \left(i \int_{\gamma} A^2 \right) + \exp \left(i \int_{\sigma} B^3 \right) + \exp \left(i \int_{\sigma} A^2 + B^3 \right) \right] \\ &= \frac{1}{\mathcal{Z}} \int \mathcal{D}[AB] \exp(iS) \times \left[\mathcal{O}_1 + \mathcal{O}_{\mathbf{P}_{010}} + \mathcal{O}_{\mathbf{L}_{001}} + \mathcal{O}_{\mathbf{L}_{001}^{010}} \right] \\ &= \langle 1 \oplus \mathbf{P}_{010} \oplus \mathbf{L}_{001} \oplus \mathbf{L}_{001}^{010} \rangle, \end{aligned} \quad (16)$$

where 1 is the vacuum, \mathbf{P}_{010} is a particle carrying a gauge charge minimally coupled to 1-form field A^2 , \mathbf{L}_{001} is a loop carrying a gauge charge minimally coupled to 2-form fields B^3 , \mathbf{L}_{001}^{010}

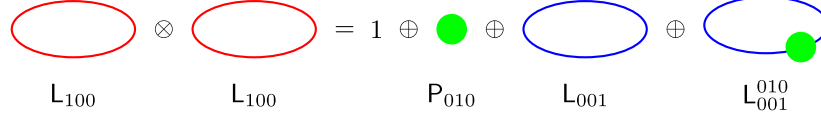


FIG. 1. A typical example of fusion rules in BF theory with AAB twisted term. Fusing two loops L_{100} has four possible fusion channels: the vacuum, the particle P_{010} , the pure loop L_{001} , and the decorated loop L_{001}^{010} .

is a decorated loop carrying both a gauge charge minimally coupled to A^2 and a gauge charge minimally coupled to B^3 . Their corresponding gauge invariant Wilson operators are [28]

$$\begin{aligned} \mathcal{O}_1 &= 1, & \mathcal{O}_{P_{010}} &= \exp\left(i \int_{\gamma} A^2\right), \\ \mathcal{O}_{L_{001}} &= \exp\left(i \int_{\sigma} B^3\right), & \mathcal{O}_{L_{001}^{010}} &= \exp\left(i \int_{\gamma} A^2 + i \int_{\sigma} B^3\right). \end{aligned} \quad (17)$$

Here, γ is the world line of particles and σ is the world sheet of loops. Eq. (16) means that fusing two loops L_{100} has four possible outputs: the vacuum, the particle P_{010} , the loop L_{001} , and the loop L_{001}^{010} . This is a non-Abelian fusion process as shown in figure 1. One fusion channel can be changed to another by braiding processes.

In 3D topological orders, topological excitations are point-like particles, i.e., anyons. However, in higher-dimensional topological orders, spatially extended topological excitations may occur. For instance, in 4D, there exist loop excitations. By applying a series of local unitary operators, we can manipulate a particle to pass through the geometric hole of the loop, which forms a particle-loop braiding process. However, such a process can only happen when the spatial size of the loop is larger than the correlation length of the TQFT. If we shrink the loop to a size that is smaller than the correlation length, no excitation can pass through the hole of the loop, causing the loop to behave like a particle when braiding with other excitations. This motivates us to consider the shrinking rules: when we shrink a spatially higher dimensional topological excitation to a sufficiently small size, it behaves like a spatially lower dimensional excitation. In 4D, there exist loop excitations and they can be shrunk to point-like particles. Keep lifting dimension to 5D, spatially extended topological excitations include both loops and membranes. Some membranes can be shrunk to loops first and then shrunk to particles, and such shrinking processes are called *hierarchical shrinking rules*. In the path integral representation, we define a shrinking operator \mathcal{S} ,

then shrinking an excitation a is [28, 29]

$$\begin{aligned}
\langle \mathcal{S}(a) \rangle &= \langle \lim_{X_1 \rightarrow X_2} a \rangle = \lim_{X_1 \rightarrow X_2} \frac{1}{\mathcal{Z}} \int \mathcal{D}[ABC] \exp(iS) \mathcal{O}_a \\
&= \sum_b \frac{1}{\mathcal{Z}} \int \mathcal{D}[ABC] \exp(iS) S_b^a \mathcal{O}_b \\
&= \langle \oplus_b S_b^a \rangle,
\end{aligned} \tag{18}$$

where \mathcal{Z} and S are partition function and action respectively. X_1 and X_2 ($X_2 \subset X_1$) are respectively spacetime trajectories (manifold) of excitation a (Wilson operator \mathcal{O}_a) before and after shrinking. We can simply rewrite eq. (18) as

$$\mathcal{S}(a) = \oplus_b S_b^a. \tag{19}$$

$S_b^a \in \mathbb{Z}$ is the shrinking coefficient, and there are S_b^a shrinking channels to b . Summation \oplus_b exhausts all topological excitations in the system. If $S_b^a = 0$, then shrinking a to b is prohibited. A shrinking process is called Abelian if it has a single shrinking channel. Otherwise, it is deemed non-Abelian. Working in the TQFT paradigm, refs. [28, 29] show that (hierarchical) shrinking rules respect fusion rules; that is, in 4D, we have:

$$\mathcal{S}(a) \otimes \mathcal{S}(b) = \mathcal{S}(a \otimes b). \tag{20}$$

Eq. (20) only holds for 4D because we only need one step to shrink loops to particles, which precludes the existence of non-trivial hierarchical shrinking structures. While in 5D, topological excitations can be particles, loops, and membranes. For a sphere-like membrane, we can directly shrink it to particles. However, for a torus-like membrane, we may first shrink it to a loop and then continue to shrink the loop to a particle. If we need at least two steps to shrink such a membrane to a particle, we say there exist hierarchical shrinking rules. Ref. [29] shows that for 5D topological order described by the BF field theory, the BBA and $AAAB$ twisted terms can lead to nontrivial hierarchical shrinking rules. For the $AAAAA$, $AAAdA$, and AAC twisted terms, we find that they have non-Abelian shrinking rules, but their shrinking rules are not hierarchical, i.e., torus-like membranes are shrunk to nontrivial particles and the trivial loop in the first step. Since the trivial loop is equivalent to the vacuum and thus can be ignored, these torus-like membranes are directly shrunk to particles in the first shrinking process. For the $AdAdA$, $AdAB$, and $AAdB$ twisted terms, they only admit Abelian shrinking rules and trivial hierarchical shrinking rules. Generally, in 5D, hierarchical shrinking rules respect fusion rules, that is,

$$\mathcal{S}^2(a) \otimes \mathcal{S}^2(b) = \mathcal{S}^2(a \otimes b), \tag{21}$$

where $\mathcal{S}^2(\cdot) = \mathcal{S}(\mathcal{S}(\cdot))$ means shrinking twice.

Following the notations in ref. [29], here we calculate an explicit example of shrinking a torus-like membrane M_{001}^T (whose Wilson operator is shown in eq. (7)) in the *BBA* twisted term:

$$\begin{aligned}
\langle \mathcal{S}(M_{001}^T) \rangle &= \langle \lim_{\omega \rightarrow \sigma} M_{001}^T \rangle = \lim_{\omega \rightarrow \sigma} \frac{1}{\mathcal{Z}} \int \mathcal{D}[ABC] \exp(iS) \times \mathcal{O}_{M_{001}^T} \\
&= \lim_{\omega \rightarrow \sigma} \frac{1}{\mathcal{Z}} \int \mathcal{D}[ABC] \exp(iS) \times 4 \exp \left[i \int_{\omega} C^3 + \frac{1}{2} \frac{2\pi q}{N_3} (d^{-1} B^1 B^2 + d^{-1} B^2 B^1) \right] \\
&\quad \times \delta \left(\int_{\sigma} B^1 \right) \delta \left(\int_{\sigma} B^2 \right) \\
&= \frac{1}{\mathcal{Z}} \int \mathcal{D}[ABC] \exp(iS) \left[1 + \exp \left(i \int_{\sigma} B^1 \right) + \exp \left(i \int_{\sigma} B^2 \right) + \exp \left(i \int_{\sigma} B^1 + i \int_{\sigma} B^2 \right) \right] \\
&= \frac{1}{\mathcal{Z}} \int \mathcal{D}[ABC] \exp(iS) [\mathcal{O}_1 + \mathcal{O}_{L_{100}} + \mathcal{O}_{L_{010}} + \mathcal{O}_{L_{110}}] \\
&= \langle 1 \oplus L_{100} \oplus L_{010} \oplus L_{110} \rangle. \tag{22}
\end{aligned}$$

Here, M_{001}^T is a torus-like membrane carrying a gauge charge minimally coupled to 3-form field C^3 . 1 is the vacuum, L_{100} , and L_{010} , are loops carrying a gauge charge minimally coupled to 2-form field B^1 and a gauge charge minimally coupled to 2-form field B^2 respectively, L_{110} , is a loop carrying both a gauge charge minimally coupled to B^1 and a gauge charge minimally coupled to B^2 . Their corresponding gauge invariant Wilson operators are [29]

$$\begin{aligned}
\mathcal{O}_1 &= 1, \quad \mathcal{O}_{L_{100}} = \exp \left(i \int_{\sigma} B^1 \right), \quad \mathcal{O}_{L_{010}} = \exp \left(i \int_{\sigma} B^2 \right) \\
\mathcal{O}_{L_{110}} &= \exp \left(i \int_{\sigma} B^1 + i \int_{\sigma} B^2 \right). \tag{23}
\end{aligned}$$

This result means that shrinking the membrane M_{001}^T has four shrinking channels: the vacuum, the loop L_{100} , the loop L_{010} , and the loop L_{110} . These loops can be further shrunk to particles, i.e., the membrane M_{001}^T have hierarchical shrinking rules:

$$\begin{aligned}
\langle \mathcal{S}^2(M_{001}^T) \rangle &= \langle \mathcal{S}(1 \oplus L_{100} \oplus L_{010} \oplus L_{110}) \rangle = \langle \lim_{\sigma \rightarrow \gamma} (1 \oplus L_{100} \oplus L_{010} \oplus L_{110}) \rangle \\
&= \lim_{\sigma \rightarrow \gamma} \frac{1}{\mathcal{Z}} \int \mathcal{D}[ABC] \exp(iS) \left[1 + \exp \left(i \int_{\sigma} B^1 \right) + \exp \left(i \int_{\sigma} B^2 \right) + \exp \left(i \int_{\sigma} B^1 + B^2 \right) \right] \\
&= \frac{1}{\mathcal{Z}} \int \mathcal{D}[ABC] \exp(iS) [1 + \exp(i0) + \exp(i0) + \exp(i0)] \\
&= \frac{1}{\mathcal{Z}} \int \mathcal{D}[ABC] \exp(iS) \times 4 \cdot 1 = \langle 4 \cdot 1 \rangle. \tag{24}
\end{aligned}$$

This result indicates that, by performing shrinking twice, M_{001}^T can be shrunk to the vacuum ultimately, as shown in figure 2.

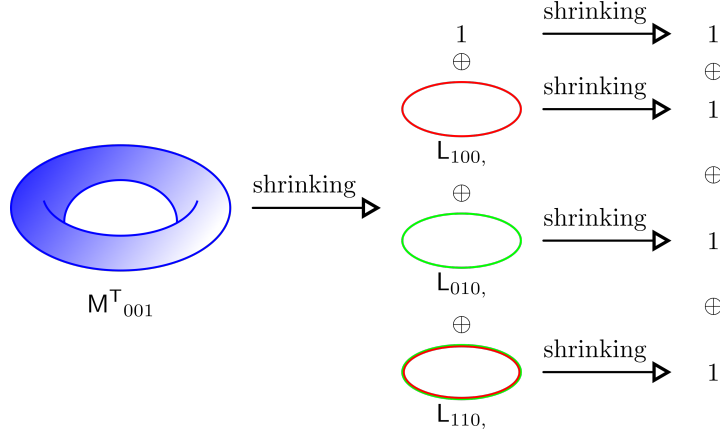


FIG. 2. A typical example of hierarchical shrinking rules in BF theory with BBA twisted term. The torus membrane M^T_{001} has four shrinking channels: the vacuum, the loop $L_{100,}$, the loop $L_{010,}$, and the loop $L_{110,}$. Subsequently, these loops are shrunk to vacua.

III. FUSION AND SHRINKING RULES AS MAPPINGS

In this section, we will categorize excitations into different sets and investigate fusion and shrinking processes as mappings between these sets. Excitations from different sets need to be treated differently in our diagrammatic representations because they play distinct roles in (hierarchical) shrinking processes. Assuming only a finite number of topologically distinct excitations exist in a topological order, we can exhaust all excitations and put them in a *set of excitations*, denoted as $\Phi_0^{\mathcal{D}}$, where the superscript \mathcal{D} denotes the spacetime dimension. In this paper, we mainly focus on $\mathcal{D} = 4, 5$. In the following discussion, we interpret shrinking as a mapping from the set $\Phi_0^{\mathcal{D}}$ to one of its subsets, denoted as $\Phi_1^{\mathcal{D}}$. If nontrivial hierarchical shrinking rules exist, we are allowed to map the subset $\Phi_i^{\mathcal{D}}$ to a smaller subset $\Phi_{i+1}^{\mathcal{D}}$, where $i = 0, 1, \dots, \mathcal{D} - 4$.

A. 4D topological orders

In a 4D topological order, we generally list all excitations in a set Φ_0^4 as follows:

$$\Phi_0^4 = \{1, P_1, P_2, \dots, P_n, L_1, L_2, \dots, L_m\}, \quad (25)$$

where 1 denotes the vacuum (both the trivial particle P_0 and trivial loop L_0 are equivalent to vacuum, i.e., $1 = P_0 = L_0$). P_i and L_i denote particles and loops respectively. The possible

outputs of fusing two excitations still form the set Φ_0^4 , thus we can regard fusion as a mapping:

$$\otimes : \Phi_0^4 \times \Phi_0^4 \rightarrow \Phi_0^4, \quad (26)$$

where $\Phi_0^4 \times \Phi_0^4 = \{(E_i, E_j) \mid E_i \in \Phi_0^4, E_j \in \Phi_0^4\}$ and the symbol \otimes means fusion.

A shrinking operator can shrink loops into particles, but it will not alter particles (which means the shrinking operator acts on a particle will give the particle itself) as, evidently, there is no way to further shrink a point. Thus, shrinking can be considered as a mapping from the original set Φ_0^4 to a subset Φ_1^4 :

$$\mathcal{S} : \Phi_0^4 \rightarrow \Phi_1^4. \quad (27)$$

$$\Phi_1^4 = \{P_0, P_1, P_2, \dots, P_n\}. \quad (28)$$

Ref. [28] shows that such a subset Φ_1^4 also has closed fusion rules, i.e., the possible outputs of fusing two excitations in Φ_1^4 still form the set Φ_1^4 . As a result, eq. (26) can be generalized to encompass the following fusion processes:

$$\otimes : \Phi_i^4 \times \Phi_i^4 \rightarrow \Phi_i^4, \quad i = 0, 1. \quad (29)$$

Now consider two copies of the set Φ_0^4 , we have two ways to map $\Phi_0^4 \times \Phi_0^4$ to the subset Φ_1^4 . The first approach involves mapping $\Phi_0^4 \times \Phi_0^4$ to Φ_0^4 by fusion, and then mapping Φ_0^4 to Φ_1^4 by shrinking. Alternatively, we can map $\Phi_0^4 \times \Phi_0^4$ to $\Phi_1^4 \times \Phi_1^4$ by shrinking, and subsequently map $\Phi_1^4 \times \Phi_1^4$ to Φ_1^4 by fusion. These two procedures can be represented as

$$(a) \quad \otimes : \Phi_0^4 \times \Phi_0^4 \rightarrow \Phi_0^4, \quad \mathcal{S} : \Phi_0^4 \rightarrow \Phi_1^4, \quad (30)$$

$$(b) \quad \mathcal{S} : \Phi_0^4 \times \Phi_0^4 \rightarrow \Phi_1^4 \times \Phi_1^4, \quad \otimes : \Phi_1^4 \times \Phi_1^4 \rightarrow \Phi_1^4, \quad (31)$$

respectively. Recall eq. (20) in 4D, shrinking rules respect fusion rules. We conclude that for $a, b \in \Phi_0^4$, $\mathcal{S}(a \otimes b)$ and $\mathcal{S}(a) \otimes \mathcal{S}(b)$ only differ by intermediate states and they give the same outputs.

In the following, we take the AAB twisted term in 4D as an example. We consider the gauge group as $G = \prod_{i=1}^n \mathbb{Z}_{N_i} = (\mathbb{Z}_2)^3$ and the action given by eq. (1). Ref. [28] shows that there are 19 distinct excitations, which form the set Φ_0^4

$$\begin{aligned} \Phi_0^4 = \{ & 1, P_{100}, P_{010}, P_{001}, P_{110}, L_{100}, L_{010}, L_{001}, L_{110}, \\ & L_{100}^{001}, L_{100}^{100}, L_{010}^{010}, L_{010}^{001}, L_{001}^{100}, L_{001}^{010}, L_{001}^{110}, L_{001}^{001}, L_{110}^{100}, L_{110}^{001} \}. \end{aligned} \quad (32)$$

Here, 1, P, and L denote the vacuum, particles, and loops respectively. Consider $n_i, m_i = 0, 1$, the subscript “ $n_1 n_2 n_3$ ” of a particle denotes that the particle carries n_1, n_2 , and n_3 gauge charges minimally coupled to the 1-form gauge fields A^1, A^2 , and A^3 , respectively. The subscript “ $n_1 n_2 n_3$ ” of a loop denotes that the loop carries n_1, n_2 , and n_3 gauge charges minimally coupled to 2-form gauge fields B^1, B^2 , and B^3 , respectively. The superscript “ $m_1 m_2 m_3$ ” of a loop denotes that the loop is decorated by m_1, m_2 , and m_3 gauge charges minimally coupled to the 1-form gauge fields A^1, A^2 , and A^3 , respectively. From ref. [28], we conclude that the subset Φ_1^4 is given by

$$\Phi_1^4 = \{1, P_{100}, P_{010}, P_{001}, P_{110}\}. \quad (33)$$

B. 5D topological orders

We can generalize the above prescription to 5D, where excitations include particles, loops, and membranes. We can generally list the set Φ_0^5 as:

$$\Phi_0^5 = \{1, P_1, P_2, \dots, P_n, L_1, L_2, \dots, L_m, M_1, M_1, \dots, M_k\}, \quad (34)$$

where 1 is the vacuum (trivial particle P_0 , trivial loop L_0 , and trivial membrane M_0 are equivalent to vacuum), P_i, L_i , and M_i denote particles, loops, and membranes respectively. If we consider nontrivial hierarchical shrinking rules, loops and membranes are shrunk to particles and loops respectively in the first shrinking process, which can be considered as a mapping from the original set Φ_0^5 to a subset Φ_1^5 :

$$\Phi_1^5 = \{1, P_1, P_2, \dots, P_n, L_1, L_2, \dots, L_p\}, \quad (35)$$

where $p \leq m$ because some loops may not appear as shrinking outputs. In fact, ref. [29] shows that we have $p < m$ for the *BBA* and *AAAB* twisted terms. (If the topological order does not have nontrivial hierarchical shrinking rules, then L_1, L_2, \dots, L_p vanish, which means that the subset Φ_1^5 and the subset Φ_2^5 [to be defined below] contain the same excitations). Continue to shrink the excitations in subset Φ_1^5 , we get a smaller subset:

$$\Phi_2^5 = \{1, P_1, P_2, \dots, P_n\}. \quad (36)$$

Given the result in ref. [29], we can verify that the sets Φ_0^5, Φ_1^5 , and Φ_2^5 all have closed fusion rules. Thus we can consider shrinking and fusion as mappings:

$$\begin{aligned} \otimes : \quad & \Phi_i^5 \times \Phi_i^5 \rightarrow \Phi_i^5, \quad i = 0, 1, 2 \\ \mathcal{S} : \quad & \Phi_j^5 \rightarrow \Phi_{j+1}^5, \quad j = 0, 1 \end{aligned} \quad (37)$$

If we consider fusion and shrinking simultaneously, we will find that the original set Φ_0^5 only admits

$$\mathcal{S}^2(a) \otimes \mathcal{S}^2(b) = \mathcal{S}^2(a \otimes b), \quad a, b \in \Phi_0^5. \quad (38)$$

While the subset Φ_1^5 and Φ_2^5 admit

$$\mathcal{S}(c) \otimes \mathcal{S}(d) = \mathcal{S}(c \otimes d), \quad c, d \in \Phi_{1,2}^5. \quad (39)$$

Eq. (39) is not the most general relation in 5D because c and d can only be particles and loops. Since the subset Φ_1^5 and Φ_2^5 can be obtained by acting a shrinking process on Φ_0^5 , i.e., we can always find $a \in \Phi_0^5$ and $b \in \Phi_0^5$ such that $\mathcal{S}(a)$ and $\mathcal{S}(b)$ have shrinking channels to $c \in \Phi_{1,2}^5$ and $d \in \Phi_{1,2}^5$ respectively, we have

$$\mathcal{S}^2(a) \otimes \mathcal{S}^2(b) = \mathcal{S}(\mathcal{S}(a) \otimes \mathcal{S}(b)) \quad (40)$$

holds for the original set Φ_0^5 . Now consider two copies of the set Φ_0^5 , we have three ways to map $\Phi_0^5 \times \Phi_0^5$ to Φ_2^5 :

$$\begin{aligned} \text{(a)} \quad \mathcal{S} &: \Phi_0^5 \times \Phi_0^5 \rightarrow \Phi_1^5 \times \Phi_1^5, \\ \mathcal{S} &: \Phi_1^5 \times \Phi_1^5 \rightarrow \Phi_2^5 \times \Phi_2^5, \\ \otimes &: \Phi_2^5 \times \Phi_2^5 \rightarrow \Phi_2^5, \end{aligned} \quad (41)$$

$$\begin{aligned} \text{(b)} \quad \otimes &: \Phi_0^5 \times \Phi_0^5 \rightarrow \Phi_0^5, \\ \mathcal{S} &: \Phi_0^5 \rightarrow \Phi_1^5, \\ \mathcal{S} &: \Phi_1^5 \rightarrow \Phi_2^5, \end{aligned} \quad (42)$$

$$\begin{aligned} \text{(c)} \quad \mathcal{S} &: \Phi_0^5 \times \Phi_0^5 \rightarrow \Phi_1^5 \times \Phi_1^5, \\ \otimes &: \Phi_1^5 \times \Phi_1^5 \rightarrow \Phi_1^5, \\ \mathcal{S} &: \Phi_1^5 \rightarrow \Phi_2^5. \end{aligned} \quad (43)$$

For $a, b \in \Phi_0^5$, the condition $\mathcal{S}^2(a) \otimes \mathcal{S}^2(b) = \mathcal{S}^2(a \otimes b) = \mathcal{S}(\mathcal{S}(a) \otimes \mathcal{S}(b))$ indicates that the three processes above only differ by intermediate states and they should give the same outputs.

Here, we take the *BBA* twisted term in 5D as an example. We consider the gauge group as $G = \prod_{i=1}^n \mathbb{Z}_{N_i} = (\mathbb{Z}_2)^3$ and the action given by eq. (3). Ref. [29] shows that there are 29 distinct excitations, which form the set Φ_0^5 (pay attention to commas and semicolons in sub- and

super-scripts):

$$\begin{aligned} \Phi_0^5 = \{ & 1, P_{001}, L_{100}, L_{010}, L_{110}, L_{100}^{001}, L_{010}^{001}, L_{110}^{001}, L_{,100}, L_{,010}, L_{,110}, L_{100,100}, L_{010,010}, L_{100,110}, \\ & M_{001}^S, M_{001}^{S,001}, M_{001}^{S,100}, M_{001}^{S,010}, M_{001}^{S,110}, M_{001}^T, M_{001}^{T,001}, M_{001}^{T,100}, M_{001}^{T,010}, M_{001}^{T,110}, M^{ST}, \\ & M^{ST,001}, M^{ST,100}, M^{ST,010}, M^{ST,110} \}. \end{aligned} \quad (44)$$

Here, 1, P, L, M^S , and M^T denote the vacuum, particles, loops, sphere-like membranes, and torus-like membranes respectively. The superscripts and subscripts are defined as follows:

- For particles, the subscript “ $n_1 n_2 n_3$ ” denotes n_1 , n_2 , and n_3 gauge charges minimally coupled to A^1 , A^2 , and A^3 , respectively.
- For loops, the superscript “ $m_1 m_2 m_3$ ” denotes m_1 , m_2 , and m_3 gauge charges minimally coupled to A^1 , A^2 , and A^3 , respectively. The subscript “ $n_1 n_2 n_3, \tilde{n}_1 \tilde{n}_2 \tilde{n}_3$ ” of loops denotes (i) n_1 , n_2 , and n_3 gauge charges minimally coupled to B^1 , B^2 , and B^3 , respectively, and (ii) \tilde{n}_1 , \tilde{n}_2 , and \tilde{n}_3 gauge charges minimally coupled to \tilde{B}^1 , \tilde{B}^2 , and \tilde{B}^3 , respectively.
- For the sake of convenience, we simply write “ $n_1 n_2 n_3, 000$ ” and “ $000, n_1 n_2 n_3$ ” as “ $n_1 n_2 n_3,$ ” and “ $, n_1 n_2 n_3$ ” respectively.
- For sphere-like and torus-like membranes, the superscript “ $p_1 p_2 p_3; m_1 m_2 m_3, \tilde{m}_1 \tilde{m}_2 \tilde{m}_3$ ” denotes (i) p_1 , p_2 , and p_3 gauge charges minimally coupled to A^1 , A^2 , and A^3 , respectively, (ii) m_1 , m_2 , and m_3 gauge charges minimally coupled to \tilde{B}^1 , \tilde{B}^2 , and \tilde{B}^3 , respectively, and (iii) \tilde{m}_1 , \tilde{m}_2 , and \tilde{m}_3 gauge charges minimally coupled to \tilde{B}^1 , \tilde{B}^2 , and \tilde{B}^3 , respectively. The subscript $n_1 n_2 n_3$ denotes n_1 , n_2 , and n_3 gauge charges minimally coupled to the 3-form gauge fields C^1 , C^2 , and C^3 , respectively.
- For the sake of convenience, we simply express “ $p_1 p_2 p_3; 000, 000$ ” and “ $000; 000, \tilde{m}_1 \tilde{m}_2 \tilde{m}_3$ ” as “ $p_1 p_2 p_3;$ ” and “ $, \tilde{m}_1 \tilde{m}_2 \tilde{m}_3$ ” respectively.

$M^{ST, n_1 n_2 n_3; m_1 m_2 m_3, p_1 p_2 p_3}$ can be generated by fusing a sphere-like M_{001}^S membrane and a torus-like membrane $M_{001}^{T, n_1 n_2 n_3; m_1 m_2 m_3, p_1 p_2 p_3}$, i.e.,

$$M^{ST, n_1 n_2 n_3; m_1 m_2 m_3, p_1 p_2 p_3} = M_{001}^S \otimes M_{001}^{T, n_1 n_2 n_3; m_1 m_2 m_3, p_1 p_2 p_3}. \quad (45)$$

The subsets Φ_1^5 and Φ_2^5 are given by

$$\Phi_1^5 = \{1, P_{001}, L_{100}, L_{010}, L_{110}, L_{100}^{001}, L_{010}^{001}, L_{110}^{001}\} \quad (46)$$

$$\Phi_2^5 = \{1, P_{001}\}. \quad (47)$$

By means of these definitions of sets, we will construct diagrammatic representations of higher-dimensional topological orders in section IV and section V.

IV. DIAGRAMMATICS OF 4D TOPOLOGICAL ORDERS

In this section, inspired by several results from TQFT, we construct diagrammatic representations of 4D topological orders that can consistently describe fusion and shrinking rules, especially focusing on unitary operators during the processes of fusion and shrinking. We obtain pentagon equations and shrinking-fusion hexagon equations for anomalous-free topological orders in 4D, which enforces constraints on legitimate unitary operators. We will generalize our construction to 5D in section V, in which the existence of membrane excitations makes hierarchical shrinking processes possible.

A. Fusion diagrams: fusion space, F -symbols, and pentagon relation

First, we explore the construction of fusion diagrams in 4D. In the following discussion, Latin and Greek letters denote excitations and channels respectively. Suppose the fusion process $a \otimes b$ has fusion channels to c , we can represent these fusion channels diagrammatically in figure 3. The solid lines can be understood as the spacetime trajectories of excitations. As mentioned in section III A, we can either fuse two excitations in the set Φ_0^4 or two excitations in the subset Φ_1^4 . Hence, we use double-line and single-line to represent excitations from the sets Φ_0^4 and Φ_1^4 respectively. $\mu = \{1, 2, \dots, N_c^{ab}\}$ labels different fusion channels to c . Notice that if $N_c^{ab} = 0$, we say diagrams in figure 3 cannot happen. The left diagrams in figure 3 can be defined as a vector $|a, b; c, \mu\rangle_0$, where different μ represent orthogonal vectors. This set of vectors $\{|a, b; c, \mu\rangle_0, \mu = 1, 2, \dots, N_c^{ab}\}$ spans a fusion space V_{0c}^{ab} with $\dim(V_{0c}^{ab}) = N_c^{ab}$. Similarly, we can define the right diagram in figure 3 as a vector $|a, b; c, \mu\rangle_1$, and the corresponding fusion space is V_{1c}^{ab} . Since these two diagrams only differ by single-lines and double-lines, we only draw the fusion diagrams for the set Φ_0^4 in the following discussion and omit the index “0” of vectors and spaces. *One can straightforwardly obtain the diagrams for set Φ_1^4 by simply replacing double-lines with single-lines.*

Now we further consider diagrams that involve more excitations. Suppose the fusion process $(a \otimes b) \otimes c$ has fusion channels to d , diagrammatically we have figure 4. Such a diagram can

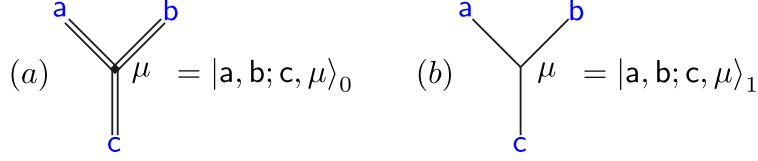


FIG. 3. Elementary fusion diagrams. a , b and c denote excitations and we highlight them in blue. $\mu = \{1, 2, \dots, N_c^{ab}\}$ labels different fusion channels with the same output c . (a) Double-lines mean that $a, b, c \in \Phi_0^4$ and this diagram represents fusion for set Φ_0^4 . (b) Single-lines mean that $a, b, c \in \Phi_1^4$ and this diagram represents fusion for set Φ_1^4 .

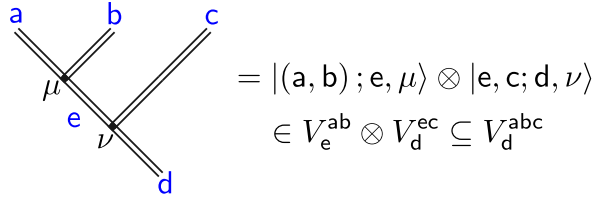


FIG. 4. Fusion diagram of three excitations. a , b , and c are input excitations, ultimately being fused into d . We highlight excitations in blue. The bracket “ (a, b) ” is added to emphasize that a and b fuse together first in the whole three-excitation fusion process. Note that, the bracket does not change the vector at all. \otimes means tensor product operation. Vectors in set $\{|(a, b); e, \mu\rangle \otimes |e, c; d, \nu\rangle\}$ span the whole space V_d^{abc} , in which different μ , ν and e label different orthogonal vectors. The space V_d^{abc} is isomorphic to $\oplus_e (V_e^{ab} \otimes V_d^{ec})$, where \oplus means direct sum. The dimension of V_d^{abc} is given by $\dim V_d^{abc} = \sum_e N_e^{ab} N_d^{ec}$. Here we only draw the diagram for fusion process in the set Φ_0^4 and simply write $|(a, b); e, \mu\rangle_0$ and V_0^{ab} as $|(a, b); e, \mu\rangle$ and V_e^{ab} respectively. One can obtain the diagram for subset Φ_1^4 by simply replacing all double-lines with single-lines.

be constructed by stacking two fusion diagrams shown in figure 3. The diagram in figure 4 can also be defined as a vector $|(a, b); e, \mu\rangle \otimes |e, c; d, \nu\rangle$, where \otimes means tensor product. The corresponding space is denoted as V_d^{abc} , whose dimension is $\dim(V_d^{abc}) = \sum_e N_e^{ab} N_d^{ec}$ because V_d^{abc} is isomorphic to $\oplus_e V_e^{ab} \otimes V_d^{ec}$.

In section III, we have discussed the crucial physical property of fusion rules known as associativity, i.e., $(a \otimes b) \otimes c = a \otimes (b \otimes c)$. This means that fusing b and c first should give the same final output as fusing a and b first. Therefore, the diagram shown in figure 5 also represents a set of basis vectors in V_d^{abc} . Actually, figure 4 and figure 5 represent different bases and we can use a unitary matrix, known as the F -symbol, to change the basis. The definition of the F -symbol is

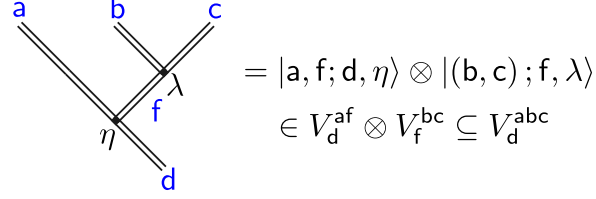


FIG. 5. A different diagram of fusing three excitations. The associativity of fusion rules guarantees that this diagram actually describes the same physics as the diagram shown in figure 4. The only difference between them is just a change of basis.

given by figure 6. We can express the equation in figure 6 as:

$$|(a, b); e, \mu\rangle \otimes |e, c; d, \nu\rangle = \sum_{f, \lambda, \eta} [F_d^{abc}]_{e\mu\nu, f\lambda\eta} |a, f; d, \eta\rangle \otimes |(b, c); f, \lambda\rangle. \quad (48)$$

The summation over f exhausts all excitations in the system, $\lambda = \{1, 2, \dots, N_f^{bc}\}$ and $\eta = \{1, 2, \dots, N_d^{af}\}$. Since the F -symbol is unitary, we have

$$\sum_{f, \lambda, \eta} [F_d^{abc}]_{e\mu\nu, f\lambda\eta} \left([F_d^{abc}]_{e'\mu'\nu', f\lambda\eta} \right)^* = \delta_{ee'} \delta_{\mu\mu'} \delta_{\nu\nu'} \quad (49)$$

which implies figure 7. We can also derive a constraint on fusion coefficients by comparing the dimension of V_d^{abc} calculated from figure 4 and figure 5, where the total space V_d^{abc} is constructed by $\oplus_e V_e^{ab} \otimes V_d^{ec}$ and $\oplus_f V_d^{af} \otimes V_f^{bc}$ respectively. Thus

$$\dim(V_d^{abc}) = \sum_e N_e^{ab} N_d^{ec} = \sum_f N_d^{af} N_f^{bc}. \quad (50)$$

This formula can also be derived by directly using associativity and eq. (11):

$$(a \otimes b) \otimes c = (\oplus_e N_e^{ab} e) \otimes c = \oplus_{ed} N_e^{ab} N_d^{ec} d, \quad (51)$$

$$a \otimes (b \otimes c) = a \otimes (\oplus_f N_f^{bc} f) = \oplus_{fd} N_f^{bc} N_d^{af} d. \quad (52)$$

Comparing the fusion coefficients, we have:

$$\sum_e N_e^{ab} N_d^{ec} = \sum_f N_d^{af} N_f^{bc}. \quad (53)$$

For other diagrams involving more excitations, we employ a similar tensor product approach to write down the corresponding vectors. Also, the F -symbols can be applied inside more complicated diagrams. For instance, consider fusing four excitations, we have different ways to transform

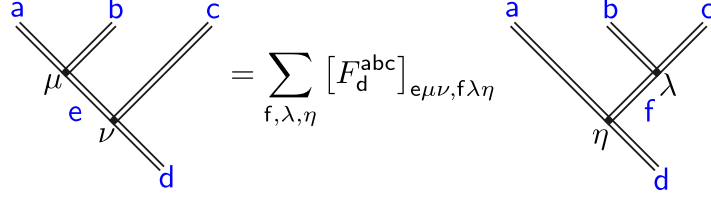


FIG. 6. Definition of the F -symbol. The left and right diagrams describe the same physics in different bases. We use the unitary F -symbol to change the basis. a , b , and c denote the inputs. d denotes the output. e , μ , ν , f , λ , and η denote different channels.

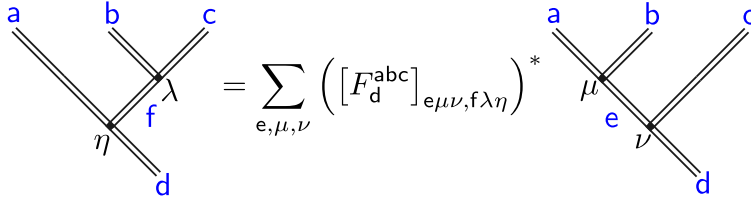


FIG. 7. Inverse transformation. This figure comes from the unitarity of the F -symbols. We use the star to denote complex conjugate.

one diagram into another. As shown in figure 8, we have two paths to transform the far left diagram into the far right diagram, imposing a very strong constraint on the F -symbols, known as the pentagon equation:

$$\sum_{\sigma=1}^{N_e^{\text{fh}}} [F_e^{\text{fcd}}]_{g\nu\lambda, h\gamma\sigma} [F_e^{\text{abh}}]_{f\mu\sigma, i\rho\delta} = \sum_j \sum_{\omega=1}^{N_g^{\text{aj}}} \sum_{\theta=1}^{N_j^{\text{bc}}} \sum_{\tau=1}^{N_i^{\text{jd}}} [F_g^{\text{abc}}]_{f\mu\nu, j\theta\omega} [F_e^{\text{ajd}}]_{g\omega\lambda, i\tau\delta} [F_i^{\text{bcd}}]_{j\theta\tau, h\gamma\rho}. \quad (54)$$

Such pentagon equation also exists in diagrammatic representations of 3D anyons. It has been proven that no more identities beyond the pentagon equation can be derived by drawing more complicated fusion diagrams in 3D. Essentially, the pentagon equation in any dimension arises from the associativity of the fusion rules, leading to the conclusion that no more identities can be derived from fusion diagrams in any dimension. As a side note, if we draw all previous fusion diagrams in a single-line fashion, our fusion diagrams then reduce to 3D anyonic fusion diagrams. A brief review of 3D anyon diagrams is shown in appendix A.

B. Shrinking diagrams: shrinking space and Δ -symbol

Suppose for $a \in \Phi_0^4$, $\mathcal{S}(a)$ has shrinking channels to $b \in \Phi_1^4$, then we define the corresponding shrinking diagram in figure 9. We use a triangle to represent the shrinking process. Note that

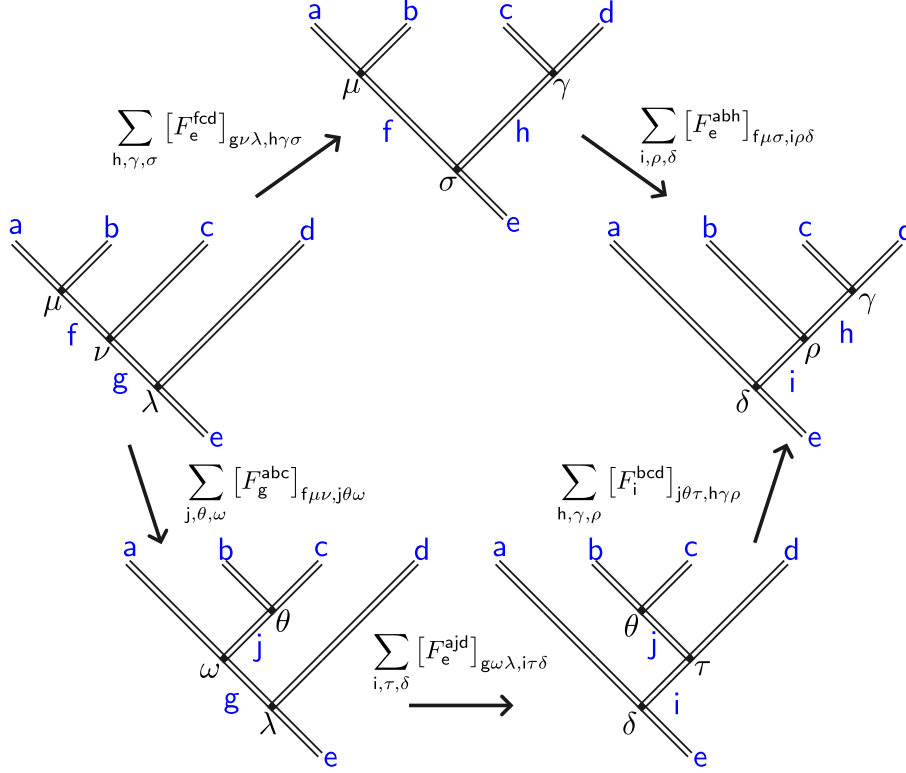


FIG. 8. Diagrammatic representation of the pentagon equation (54). We highlight the excitations in blue. Starting from the far left diagram, we can go to the far right diagram through either the upper path or the lower path. Comparing these two different paths, we can derive the pentagon equation.

in a specific diagram, a double-line and a single-line may actually represent the same particle. However, they carry distinct meanings: the double-line means that this particle from Φ_0^4 is treated as the input of the shrinking process while the single-line means that this particle from Φ_1^4 is the output. Similar to the fusion diagram, the shrinking diagram in figure 9 can be understood as a vector $|a; b, \mu\rangle$. The orthogonal set $\{|a; b, \mu\rangle, \mu = 1, 2, \dots, S_b^a\}$ spans a shrinking space V_b^a , whose dimension is $\dim(V_b^a) = S_b^a$.

Now we use tensor product to incorporate fusion and shrinking processes in a diagram. Consider $\mathcal{S}(a) \otimes \mathcal{S}(b)$ and $\mathcal{S}(a \otimes b)$, their corresponding diagrams are shown as the upper diagram and the lower diagram in figure 10 respectively. Recall eq. (20), shrinking rules respect fusion rules. Thus, if $\mathcal{S}(a) \otimes \mathcal{S}(b)$ finally gives c , then $\mathcal{S}(a \otimes b)$ must also give c . Although these two processes have the same final output, they experience different intermediate steps. For the upper diagram in figure 10, a and b shrink to d and e in the μ and ν channels respectively first, then d and e fuse to c in the λ channel. In a non-Abelian case, different legitimate choices of d , e , μ , ν , and λ

$$\begin{array}{c}
\text{a} \\
\parallel \\
\mu \swarrow \downarrow \searrow \\
\text{b}
\end{array}
= |\text{a}; \text{b}, \mu\rangle \in V_{\text{b}}^{\text{a}}, \mu \in \{1, 2, \dots, S_{\text{b}}^{\text{a}}\}$$

$$\dim(V_{\text{b}}^{\text{a}}) = S_{\text{b}}^{\text{a}}$$

FIG. 9. Shrinking diagram. According to the definition at the beginning of section IV A, the double-line and single-line represent excitations from Φ_0^4 and Φ_1^4 respectively. Here, $\text{a} \in \Phi_0^4$ is the input of the shrinking process and thus a can be a loop or a particle. $\text{b} \in \Phi_1^4$ is the output of the shrinking process and thus b can only be a particle. We use a triangle to represent the shrinking process. This diagram describes shrinking a to b in the μ channel and we define it as a vector. The orthogonal set $\{|\text{a}; \text{b}, \mu\rangle, \mu = 1, 2, \dots, S_{\text{b}}^{\text{a}}\}$ spans the shrinking space V_{b}^{a} with $\dim(V_{\text{b}}^{\text{a}}) = S_{\text{b}}^{\text{a}}$.

may exist, i.e. they can finally produce c . We define such diagram as $|\text{d}, \text{e}; \text{c}, \lambda\rangle \otimes |\text{b}; \text{e}, \nu\rangle \otimes |\text{a}; \text{d}, \mu\rangle$. Since a , b and c are already fixed, different d , e , μ , ν , and λ label different vectors. By exhausting all possible d , e , μ , ν , and λ , we obtain a set of orthogonal vectors and they span a space denoted as $V_c^{\mathcal{S}(\text{a}) \otimes \mathcal{S}(\text{b})}$, which is isomorphic to $\bigoplus_{\text{de}} V_c^{\text{de}} \otimes V_e^{\text{b}} \otimes V_d^{\text{a}}$ due to our tensor product construction. For the lower diagram in figure 10, a and b fuse to f in the δ channel first, then f shrinks to c in the γ channel. We define such diagram as $|\text{f}; \text{c}, \gamma\rangle \otimes |\text{a}, \text{b}; \text{f}, \delta\rangle$. Similarly, a , b , and c are fixed. Different legitimate choices of f , δ , and γ may exist, which label different orthogonal vectors. By exhausting all possible f , δ , and γ , we obtain a set of vectors spanning the space $V_c^{\mathcal{S}(\text{a} \otimes \text{b})}$, which is isomorphic to $\bigoplus_{\text{f}} V_c^{\text{f}} \otimes V_f^{\text{ab}}$. The conclusion that shrinking rules respect fusion rules also implies that the space $V_c^{\mathcal{S}(\text{a}) \otimes \mathcal{S}(\text{b})}$ is isomorphic to $V_c^{\mathcal{S}(\text{a} \otimes \text{b})}$, leading to:

$$\dim(V_c^{\mathcal{S}(\text{a}) \otimes \mathcal{S}(\text{b})}) = \dim(V_c^{\mathcal{S}(\text{a} \otimes \text{b})}) = \sum_{\text{de}} N_c^{\text{de}} S_e^{\text{b}} S_d^{\text{a}} = \sum_{\text{f}} S_c^{\text{f}} N_f^{\text{ab}}. \quad (55)$$

Eq. (55) can also be found in ref. [28] where all fusion and shrinking rules in the BF theory with the AAB twisted term are obtained. Also, eq. (55) is numerically verified. This constraint on fusion coefficients and shrinking coefficients can be considered as a consistency condition for fusion rules and shrinking rules in anomaly-free 4D topological orders.

The two sets of vectors shown in figure 10 are two different bases of the total space $V_c^{\mathcal{S}(\text{a}) \otimes \mathcal{S}(\text{b})}$ (or equivalently, we can write $V_c^{\mathcal{S}(\text{a} \otimes \text{b})}$ here). We expect that these two bases can transform to each other by a unitary matrix, called the Δ -symbol. The definition of the Δ -symbol is shown in

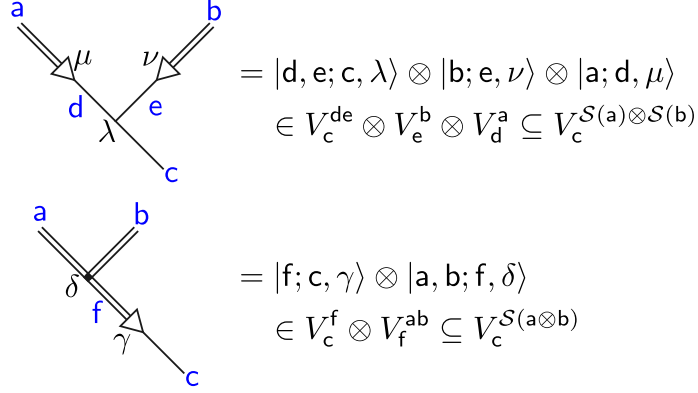


FIG. 10. Elementary diagrams that incorporate both fusion and shrinking processes. The upper diagram describes $\mathcal{S}(a) \otimes \mathcal{S}(b)$, while the lower diagram describes $\mathcal{S}(a \otimes b)$. These diagrams can be constructed by tensoring smaller diagrams. Thus, we have $V_c^{\mathcal{S}(a) \otimes \mathcal{S}(b)} \cong \oplus_{de} V_c^{de} \otimes V_e^b \otimes V_d^a$ and $V_c^{\mathcal{S}(a \otimes b)} \cong \oplus_f V_c^f \otimes V_f^{ab}$. Here, \otimes means tensor product, \oplus means direct sum, and \cong means isomorphism. We can verify that $\dim(V_c^{\mathcal{S}(a) \otimes \mathcal{S}(b)}) = \sum_{de} N_c^{de} S_e^b S_d^a$ and $\dim(V_c^{\mathcal{S}(a \otimes b)}) = \sum_f S_c^f N_f^{ab}$.

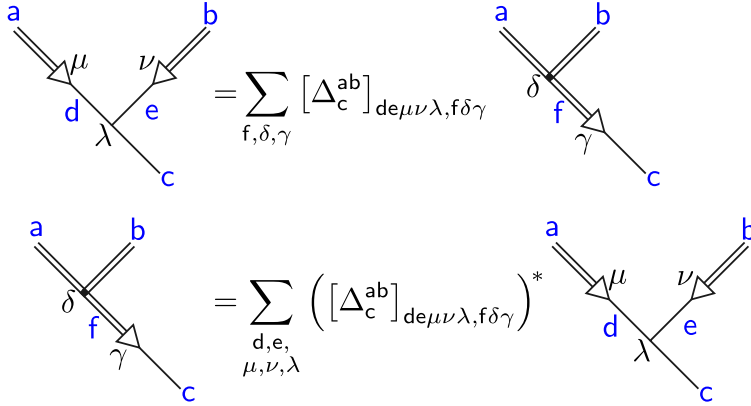


FIG. 11. Definition of the Δ -symbol. The left diagram and the right diagram describe the same physics in different bases. Similar to the F -symbol, the Δ -symbol is also unitary and we can use it to change bases. a and b denote the inputs. c denotes the output. $d, e, \mu, \nu, \lambda, f, \delta,$ and γ denote different shrinking channels.

figure 11. We can explicitly write down the transformations in figure 11 as:

$$|d, e; c, \lambda\rangle \otimes |b; e, \nu\rangle \otimes |a; d, \mu\rangle = \sum_{f, \delta, \gamma} [\Delta_c^{ab}]_{de\mu\nu\lambda, f\delta\gamma} |f; c, \gamma\rangle \otimes |a, b; f, \delta\rangle, \quad (56)$$

$$|f; c, \gamma\rangle \otimes |a, b; f, \delta\rangle = \sum_{\substack{d, e, \\ \mu, \nu, \lambda}} \left([\Delta_c^{ab}]_{de\mu\nu\lambda, f\delta\gamma} \right)^* |d, e; c, \lambda\rangle \otimes |b; e, \nu\rangle \otimes |a; d, \mu\rangle. \quad (57)$$

Unitarity of the Δ -symbol demands:

$$\sum_{f,\delta,\gamma} [\Delta_c^{ab}]_{de\mu\nu\lambda,f\delta\gamma} \left([\Delta_c^{ab}]_{d'e'\mu'\nu'\lambda',f\delta\gamma} \right)^* = \delta_{dd'} \delta_{ee'} \delta_{\mu\mu'} \delta_{\nu\nu'} \delta_{\lambda\lambda'} , \quad (58)$$

$$\sum_{\substack{d,e, \\ \mu,\nu,\lambda}} [\Delta_c^{ab}]_{de\mu\nu\lambda,f\delta\gamma} \left([\Delta_c^{ab}]_{de\mu\nu\lambda,f'\delta'\gamma'} \right)^* = \delta_{ff'} \delta_{\delta\delta'} \delta_{\gamma\gamma'} . \quad (59)$$

The element of the Δ -symbol $[\Delta_c^{ab}]_{de\mu\nu\lambda,f\delta\gamma}$ is zero if the corresponding diagram is not allowed. Although we only use diagrams that involve shrinking and fusing two excitations to define the Δ -symbol, we are allowed to act a Δ -symbol on a part of a larger diagram, such as the diagram shown in figure 12.

C. Shrinking-fusion hexagon equation

In 4D, fusion rules in both set Φ_0^4 and subset Φ_1^4 are closed and satisfy the associativity: $(a \otimes b) \otimes c = a \otimes (b \otimes c)$, which means we can use the F -symbols to change the bases when we consider diagrams involve fusing three excitations, regardless of which set do these excitations come from. We conclude that by applying the F -symbols and Δ -symbols inside of diagrams involving three excitations, we can obtain another consistency relation called the shrinking-fusion hexagon equation besides the pentagon equation. As shown in figure 12, both the upper and lower paths can transform the far left diagram (i.e., $(\mathcal{S}(a) \otimes \mathcal{S}(b)) \otimes \mathcal{S}(c)$) to the far right diagram (i.e., $\mathcal{S}(a \otimes (b \otimes c))$), these two paths correspond to:

$$\text{far left} = \sum_{\substack{i,\alpha,\beta,j, \\ \tau,\xi,k,\theta,\epsilon}} [F_d^{efg}]_{h\delta\gamma,i\alpha\beta} [\Delta_i^{bc}]_{fg\nu\lambda\alpha,j\tau\xi} [\Delta_d^{aj}]_{ei\mu\xi\beta,k\theta\epsilon} \text{ far right} , \quad (60)$$

$$\text{far left} = \sum_{\substack{t,\sigma,\rho,k, \\ \omega,\epsilon,j,\tau,\theta}} [\Delta_h^{ab}]_{ef\mu\nu\delta,t\sigma\rho} [\Delta_d^{tc}]_{hg\rho\lambda\gamma,k\omega\epsilon} [F_k^{abc}]_{t\sigma\omega,j\tau\theta} \text{ far right} , \quad (61)$$

respectively. Notice that the far right diagram is labeled by j, k, τ, θ , and ϵ . By comparing the coefficients of the far right diagrams in eq. (60) and eq. (61), we obtain a constraint on both the F -symbols and Δ -symbols:

$$\begin{aligned} & \sum_i \sum_{\alpha=1}^{N_i^{fg}} \sum_{\beta=1}^{N_d^{ei}} \sum_{\xi=1}^{S_i^j} [F_d^{efg}]_{h\delta\gamma,i\alpha\beta} [\Delta_i^{bc}]_{fg\nu\lambda\alpha,j\tau\xi} [\Delta_d^{aj}]_{ei\mu\xi\beta,k\theta\epsilon} \\ &= \sum_t \sum_{\sigma=1}^{N_t^{ab}} \sum_{\rho=1}^{S_h^t} \sum_{\omega=1}^{N_k^{tc}} [\Delta_h^{ab}]_{ef\mu\nu\delta,t\sigma\rho} [\Delta_d^{tc}]_{hg\rho\lambda\gamma,k\omega\epsilon} [F_k^{abc}]_{t\sigma\omega,j\tau\theta} . \end{aligned} \quad (62)$$

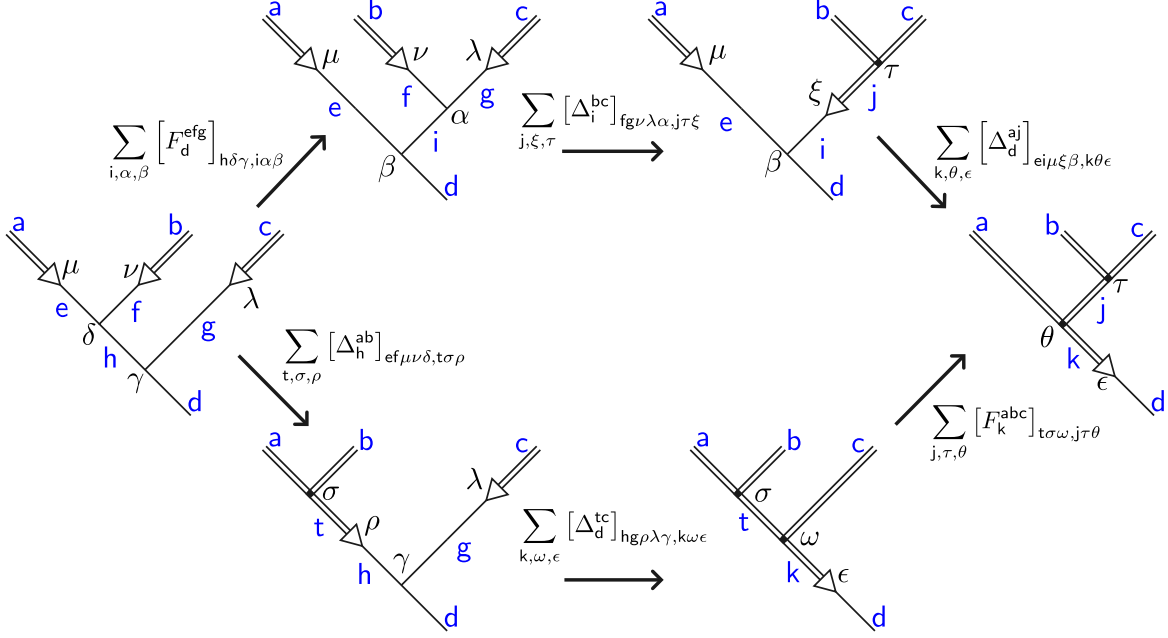


FIG. 12. Diagrammatic representations of the shrinking-fusion hexagon equation (62). Two different paths can be constructed to transform the far left diagram to the far right diagram. Comparing these two different paths, we obtain the shrinking-fusion hexagon equation.

Diagrammatically represented by figure 12, this shrinking-fusion hexagon equation can be understood as the consistency relation between the F -symbols and Δ -symbols. Since being able to use the Δ -symbols to change basis requires the consistency relation between fusion and shrinking coefficients (i.e., eq. (55) holds), we conclude that the shrinking-fusion hexagon equation actually implies eq. (55). Therefore, the shrinking-fusion hexagon equation is a stronger constraint on consistent fusion and shrinking rules, describing not only the behavior of fusion and shrinking coefficients but also the transformations of bases. We conjecture that such a shrinking-fusion hexagon is universal. All anomaly-free 4D topological orders should have consistent fusion and shrinking rules, thus satisfying this equation.

We can further consider applying the F -symbols and Δ -symbols inside of diagrams involving more excitations, such as starting from the diagram for $\mathcal{S}(a) \otimes \mathcal{S}(b) \otimes \mathcal{S}(c) \otimes \mathcal{S}(d)$ and then implementing basis transformations. However, we can verify that no more independent equations can be obtained from the diagram involving four excitations. Details can be found in appendix B. We further conjecture that no more independent equations can be obtained from diagrams involving more excitations.

$$\begin{array}{l}
a \\
\parallel \\
\mu \\
\text{b} \\
\nu \\
\text{c}
\end{array}
= |b; c, \nu\rangle \otimes |a; b, \mu\rangle \in V_c^b \otimes V_b^a \subseteq V^{\text{total}}$$

$$V^{\text{total}} \cong \bigoplus_b V_c^b \otimes V_b^a$$

$$\dim(V^{\text{total}}) = \dim(\bigoplus_b V_c^b \otimes V_b^a) = \sum_b S_c^b S_b^a$$

FIG. 13. Hierarchical shrinking diagram. The triangle represents the shrinking process. The triple-line, double-line, and single-line represent excitations in the sets Φ_0^5 , Φ_1^5 , and Φ_2^5 respectively. This diagram describes the process where the excitation a is shrunk to b in the μ channel first, followed by the further shrinking of b to c in the ν channel. The whole diagram can be considered as a vector in the total shrinking space, which is isomorphic to $\bigoplus_b V_c^b \otimes V_b^a$. Different ways for shrinking a to c correspond to different b , μ , and ν , thus correspond to different orthogonal vectors.

V. DIAGRAMMATICS OF 5D TOPOLOGICAL ORDERS

The idea of constructing the diagrammatic representations of 4D topological orders can be generalized to 5D, where nontrivial hierarchical shrinking rules may appear. An anomaly-free 5D topological order should have consistent fusion and shrinking rules. If there exist nontrivial hierarchical shrinking rules, we further demand that such hierarchical shrinking rules are also consistent with fusion and shrinking rules, which leads to the hierarchical shrinking-fusion hexagon.

A. Fusion diagrams

The construction of fusion diagrams in section IV A can be easily generalized to 5D. We can simply replace double-lines with triple-lines in the previous fusion diagrams to represent fusing two excitations in the set Φ_0^5 (see eq. (34)). Double-lines and single-lines in 5D represent excitations from the subset Φ_1^5 and Φ_2^5 respectively. The definitions of the F -symbols and the pentagon equation in section IV A remain valid. Figure 6, 7, and 8 can be drawn in triple-, double- and single-line fashions.

B. Hierarchical shrinking diagrams and Δ^2 -symbols

Suppose a has nontrivial hierarchical shrinking rules and $\mathcal{S}^2(a)$ gives c finally. We can define the corresponding hierarchical shrinking diagram in figure 13. Here, the triangle denotes the shrinking process. The triple-line, double-line, and single-line represent excitations in the sets Φ_0^5 , Φ_1^5 , and Φ_2^5 respectively. Similar to the case in 4D, although these three kinds of lines may represent the same excitation in a specific diagram, they carry different meanings, implying different roles (input or output) in a hierarchical shrinking process. The diagram in figure 13 can be understood as a vector $|b; c, \nu\rangle \otimes |a; b, \mu\rangle$. Generally, there are various legitimate choices for b , μ , and ν that can finally give the desired output c . Thus, different b , μ , and ν label different orthogonal vectors. The orthogonal set $\{|b; c, \nu\rangle \otimes |a; b, \mu\rangle\}$ spans the total shrinking space V^{total} . This total shrinking space is isomorphic to $\oplus_b V_c^b \otimes V_b^a$. Therefore, we can calculate its dimension as:

$$\dim(V^{\text{total}}) = \dim(\oplus_b V_c^b \otimes V_b^a) = \sum_b S_c^b S_b^a. \quad (63)$$

Having defined the hierarchical shrinking diagram, we can further consider representing $\mathcal{S}^2(a) \otimes \mathcal{S}^2(b)$, $\mathcal{S}^2(a \otimes b)$ and $\mathcal{S}(\mathcal{S}(a) \otimes \mathcal{S}(b))$ diagrammatically. As shown in figure 14, we stack the shrinking diagrams and fusion diagrams to describe the processes above. These diagrams are still understood as vectors and they can be constructed by tensor product. Since in 5D, hierarchical shrinking rules respect fusion rules: $\mathcal{S}^2(a) \otimes \mathcal{S}^2(b) = \mathcal{S}^2(a \otimes b)$, we can expect that the diagrams for $\mathcal{S}^2(a) \otimes \mathcal{S}^2(b)$ and $\mathcal{S}^2(a \otimes b)$ describe the same physics. Also, as mentioned in section III B, for particles and loops, the relation $\mathcal{S}(c) \otimes \mathcal{S}(d) = \mathcal{S}(c \otimes d)$ still holds. In 5D, for any excitation $c \in \Phi_1^5$, we can always find an $a \in \Phi_0^5$ such that $\mathcal{S}(a)$ has shrinking channels to c . Thus, we can replace c and d with $\mathcal{S}(a)$ and $\mathcal{S}(b)$ respectively and obtain $\mathcal{S}^2(a) \otimes \mathcal{S}^2(b) = \mathcal{S}(\mathcal{S}(a) \otimes \mathcal{S}(b))$. Similarly, we expect that the diagrams for $\mathcal{S}(\mathcal{S}(a) \otimes \mathcal{S}(b))$ describe the same physics as $\mathcal{S}^2(a) \otimes \mathcal{S}^2(b)$. Now we can say that the three diagrams shown in figure 14 correspond to three different bases of the space $V_c^{\mathcal{S}^2(a) \otimes \mathcal{S}^2(b)}$. We can calculate the dimension of $V_c^{\mathcal{S}^2(a) \otimes \mathcal{S}^2(b)}$ from these three diagrams as:

$$(a) \dim(V_c^{\mathcal{S}^2(a) \otimes \mathcal{S}^2(b)}) = \dim(\oplus_{defg} V_c^{fg} \otimes V_g^e \otimes V_e^b \otimes V_f^d \otimes V_d^a) = \sum_{defg} N_c^{fg} S_g^e S_e^b S_f^d S_d^a, \quad (64)$$

$$(b) \dim(V_c^{\mathcal{S}^2(a) \otimes \mathcal{S}^2(b)}) = \dim(\oplus_{hi} V_c^i \otimes V_i^h \otimes V_h^{ab}) = \sum_{hi} N_h^{ab} S_c^i S_i^h, \quad (65)$$

$$(c) \dim(V_c^{\mathcal{S}^2(a) \otimes \mathcal{S}^2(b)}) = \dim(\oplus_{dej} V_c^j \otimes V_j^{de} \otimes V_e^b \otimes V_d^a) = \sum_{dej} N_j^{de} S_c^j S_e^b S_d^a. \quad (66)$$

(a) $= |f, g; c, \eta\rangle \otimes |e; g, \sigma\rangle \otimes |b; e, \nu\rangle \otimes |d; f, \rho\rangle \otimes |a; d, \mu\rangle$
 $\in V_c^{fg} \otimes V_g^e \otimes V_e^b \otimes V_f^d \otimes V_d^a \subseteq V_c^{\mathcal{S}^2(a) \otimes \mathcal{S}^2(b)}$

(b) $= |i; c, \omega\rangle \otimes |h; i, \tau\rangle \otimes |a, b; h, \lambda\rangle \in V_c^i \otimes V_i^h \otimes V_h^{ab}$

(c) $= |j; c, \beta\rangle \otimes |d, e; j, \alpha\rangle \otimes |b; e, \nu\rangle \otimes |a; d, \mu\rangle$
 $\in V_c^j \otimes V_j^{de} \otimes V_e^b \otimes V_d^a$

FIG. 14. Diagrams for $\mathcal{S}^2(a) \otimes \mathcal{S}^2(b)$, $\mathcal{S}^2(a \otimes b)$ and $\mathcal{S}(\mathcal{S}(a) \otimes \mathcal{S}(b))$. These diagrams are understood as vectors. (a) Diagram for $\mathcal{S}^2(a) \otimes \mathcal{S}^2(b)$. Different $d, e, f, g, \mu, \nu, \rho, \sigma$, and η label different orthogonal vectors in the whole space $V_c^{\mathcal{S}^2(a) \otimes \mathcal{S}^2(b)}$, which is isomorphic to $\oplus_{defg} V_c^{fg} \otimes V_g^e \otimes V_e^b \otimes V_f^d \otimes V_d^a$. (b) Diagram for $\mathcal{S}^2(a \otimes b)$. Different h, i, λ, τ , and ω label different orthogonal vectors. The tensor product construction in this diagram indicates that the whole space $V_c^{\mathcal{S}^2(a) \otimes \mathcal{S}^2(b)}$ is isomorphic to $\oplus_{hi} V_c^i \otimes V_i^h \otimes V_h^{ab}$. (c) Diagram for $\mathcal{S}(\mathcal{S}(a) \otimes \mathcal{S}(b))$. Different $d, e, j, \mu, \nu, \alpha$, and β label different orthogonal vectors. The tensor product construction in this diagram indicates that the whole space is isomorphic to $\oplus_{dej} V_c^j \otimes V_j^{de} \otimes V_e^b \otimes V_d^a$.

Thus we have:

$$\sum_{defg} N_c^{fg} S_g^e S_e^b S_f^d S_d^a = \sum_{hi} N_h^{ab} S_c^i S_i^h = \sum_{dej} N_j^{de} S_c^j S_e^b S_d^a. \quad (67)$$

Eq. (67) is the consistent condition for fusion and shrinking coefficients in 5D topological orders [29].

Now we consider using unitary matrices to change bases. Since generally $\mathcal{S}(a) \otimes \mathcal{S}(b) = \mathcal{S}(a \otimes b)$ does not hold for all excitations in 5D, we need to introduce a new set of unitary matrices: the Δ^2 -symbols as shown in figure 15, to transform from the diagram for $\mathcal{S}^2(a) \otimes \mathcal{S}^2(b)$ to the diagram for $\mathcal{S}^2(a \otimes b)$. Note that the Δ^2 -symbol is not the product of two Δ -symbols. The number 2 in Δ^2 means that there are two successive shrinking processes. Generally, hierarchical shrinking rules and fusion rules in an \mathcal{D} -dimensional may satisfy $\mathcal{S}^{\mathcal{D}-3}(a) \otimes \mathcal{S}^{\mathcal{D}-3}(b) = \mathcal{S}^{\mathcal{D}-3}(a \otimes b)$. In such a scenario, the symbol that transforms from the diagram for $\mathcal{S}^{\mathcal{D}-3}(a) \otimes \mathcal{S}^{\mathcal{D}-3}(b)$ to the dia-

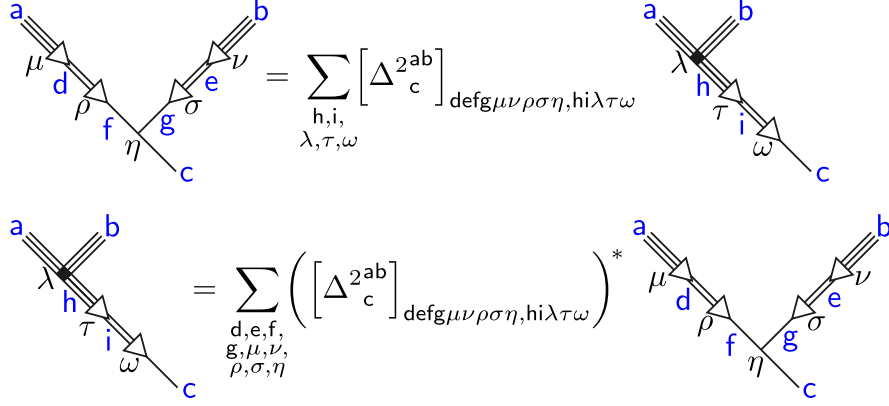


FIG. 15. Definition of Δ^2 -symbols. The left and right diagrams describe the same physics in different bases. We can use a unitary Δ^2 -symbol to change bases. “2” means that the diagrams involve hierarchical shrinking processes.

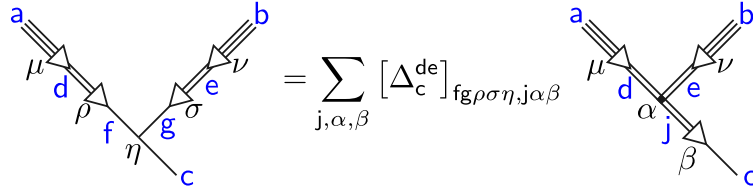


FIG. 16. Basis transformation from $\mathcal{S}^2(a) \otimes \mathcal{S}^2(b)$ to $\mathcal{S}(\mathcal{S}(a) \otimes \mathcal{S}(b))$. Since d and e can only be loops and particles, we are allowed to use the Δ -symbol to change the basis.

gram for $\mathcal{S}^{\mathcal{D}-3}(a \otimes b)$ is denoted as the $\Delta^{\mathcal{D}-3}$ -symbol. In this convention, Δ^1 -symbol is nothing but Δ -symbol. Unitarity of the Δ^2 -symbol demands:

$$\sum_{\substack{d,e,f,g, \\ \mu,\nu,\rho,\sigma,\eta}} \left[\Delta_c^{2ab} \right]_{\text{defg}\mu\nu\rho\sigma\eta, \text{hi}\lambda\tau\omega} \left(\left[\Delta_c^{2ab} \right]_{\text{defg}\mu\nu\rho\sigma\eta, \text{h}'\text{i}'\lambda'\tau'\omega'} \right)^* = \delta_{\text{hh}'} \delta_{\text{ii}'} \delta_{\lambda\lambda'} \delta_{\tau\tau'} \delta_{\omega\omega'}, \quad (68)$$

$$\sum_{\substack{h,i, \\ \lambda,\tau,\omega}} \left[\Delta_c^{2ab} \right]_{\text{defg}\mu\nu\rho\sigma\eta, \text{hi}\lambda\tau\omega} \left(\left[\Delta_c^{2ab} \right]_{\text{d}'\text{e}'\text{f}'\text{g}'\mu'\nu'\rho'\sigma'\eta'}, \text{hi}\lambda\tau\omega} \right)^* = \delta_{\text{dd}'} \delta_{\text{ee}'} \delta_{\text{ff}'} \delta_{\text{gg}'} \delta_{\mu\mu'} \delta_{\nu\nu'} \delta_{\rho\rho'} \delta_{\sigma\sigma'} \delta_{\eta\eta'}. \quad (69)$$

As for changing bases from $\mathcal{S}^2(a) \otimes \mathcal{S}^2(b)$ to $\mathcal{S}(\mathcal{S}(a) \otimes \mathcal{S}(b))$, we can still use the Δ -symbols shown in figure 11 because even in 5D, loops and particles still obey $\mathcal{S}(c) \otimes \mathcal{S}(d) = \mathcal{S}(c \otimes d)$. Thus, as shown in figure 16 and 17, we establish the basis transformations between the three diagrams in figure 14.

$$\begin{aligned}
& \text{Diagram (a,b,c)} = \sum_{\substack{d,e,f,g,h,i,j,k,l,m,n, \\ \nu,\rho,\sigma,\eta,\alpha,\beta}} \left(\left[\Delta_c^{2ab} \right]_{\text{defg}\mu\nu\rho\sigma\eta,hi\lambda\tau\omega} \right)^* \left[\Delta_c^{de} \right]_{\text{fg}\rho\sigma\eta,j\alpha\beta} \text{Diagram (d,e,f)}
\end{aligned}$$

FIG. 17. Basis transformation from $\mathcal{S}^2(a \otimes b)$ to $\mathcal{S}(\mathcal{S}(a) \otimes \mathcal{S}(b))$. We can derive this transformation by using the lower diagram in figure 15 and then use figure 16.

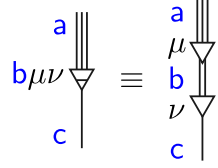


FIG. 18. Hierarchical shrinking diagram in a more compact form. We introduce the diagram on the left hand side as the simplified hierarchical shrinking diagram. Physically, this simplified diagram retains all the essential information. The triangle with a line represents the complete hierarchical shrinking process.

C. Diagrammatics of the hierarchical shrinking-fusion hexagon equation

Before investigating into diagrams where three excitations together undergo shrinking and fusion processes, we present a more compact version of figure 13, as shown in figure 18. We use a triangle decorated by a line inside the triangle, in order to represent the whole hierarchical shrinking process. If we only consider using the Δ^2 -symbols and F -symbols, it is convenient to use such a compact fashion.

Recall the figure 12, where three excitations undergo shrinking and fusion processes to finally get a particle. By using the F -symbols and Δ -symbols, we transform diagrams from each other and finally derive the shrinking-fusion hexagon equation in 4D. Now, we generalize it to 5D by substituting the Δ -symbols with the Δ^2 -symbols and employing the compact hierarchical shrinking diagrams shown in figure 18. The resulting diagram shown in figure 19 gives the hierarchical shrinking-fusion hexagon equation in 5D. The transformation from the far left diagram to the far right diagram differs along the upper and lower paths. By comparing the coefficients of the far

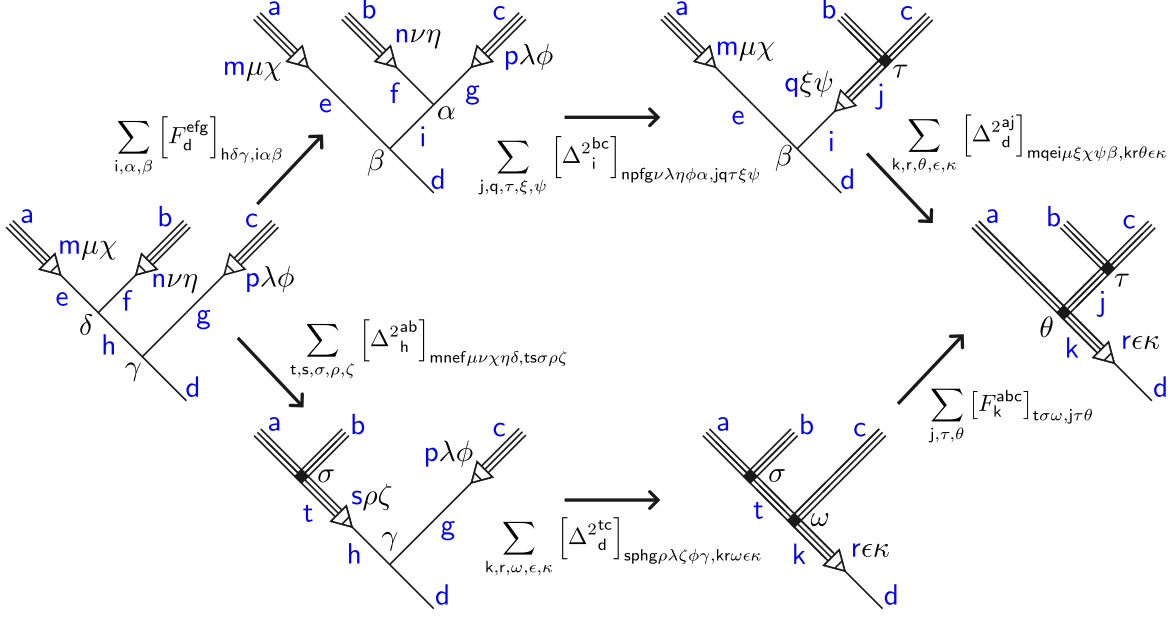


FIG. 19. Diagrammatic representations of the hierarchical shrinking-fusion hexagon equation. Here we use compact hierarchical shrinking diagrams shown in figure 18. Similar to figure 12, we have two different paths to transform the far left diagram to the far right diagram. Comparing these two different paths, we obtained the hierarchical shrinking-fusion hexagon equation.

right diagram, we derive the hierarchical shrinking-fusion hexagon equation:

$$\begin{aligned}
& \sum_{i,q} \sum_{\alpha=1}^{N_i^{fg}} \sum_{\beta=1}^{N_d^{ei}} \sum_{\xi=1}^{S_q^j} \sum_{\psi=1}^{S_i^q} [F_d^{efg}]_{h\delta\gamma, i\alpha\beta} [\Delta_i^{2bc}]_{npfg\nu\lambda\eta\phi\alpha, jq\tau\xi\psi} [\Delta_d^{2aj}]_{mqei\mu\xi\chi\psi\beta, kr\theta\epsilon\kappa} \\
&= \sum_{t,s} \sum_{\sigma=1}^{N_t^{ab}} \sum_{\omega=1}^{N_k^{tc}} \sum_{\rho=1}^{S_s^t} \sum_{\zeta=1}^{S_h^s} [\Delta_h^{2ab}]_{mnef\mu\nu\chi\eta\delta, ts\rho\zeta} [\Delta_d^{2tc}]_{sphg\rho\lambda\zeta\phi\gamma, kr\omega\epsilon\kappa} [F_k^{abc}]_{t\sigma\omega, j\tau\theta}. \quad (70)
\end{aligned}$$

Eq. (70) can be understood as the consistency relation between the F -symbols and Δ^2 -symbols.

If we do not utilize the compact diagram in figure 18, we can consider using the Δ -symbols in figure 19. In this case, we will find that shrinking-fusion hexagon (62) still holds. However, it is noteworthy that now a, b and c in eq. (62) can only belong to the subset Φ_1^5 . Such shrinking-fusion hexagon equation with a constraint on inputs is the consistency relation between the F -symbols and Δ -symbols in 5D.

Eq. (70) and eq. (62) with constrained inputs are the key results in our 5D diagrammatic representations. They establish the consistency relation between the F -symbols, Δ -symbols, and Δ^2 -symbols. They also imply constraints on fusion and shrinking coefficients, i.e., eq. (67). We

conjecture that all anomaly-free 5D topological orders should satisfy these two hexagon equations, ensuring consistent fusion, shrinking, and hierarchical shrinking rules.

VI. SUMMARY AND OUTLOOK

In this paper, with the help of our previous work on field-theoretical description of higher dimensional topological orders, we have successfully constructed diagrammatic representations for higher-dimensional topological orders in 4D and 5D spacetime, extending the framework known for topologically ordered phases in 3D spacetime. By introducing and manipulating basic fusion and shrinking diagrams as vectors within corresponding spaces, we have demonstrated the construction of complex diagrams through their stacking. Using the F -, Δ -, and Δ^2 -symbols, we have established unitary transformations between different bases in these vector spaces and discovered key consistency conditions, including the pentagon equations and (hierarchical) shrinking-fusion hexagon equations. Our findings indicate that these consistency conditions are essential for ensuring the anomaly-free nature of higher-dimensional topological orders. Violations of these conditions suggest the presence of quantum anomalies, providing a diagnostic tool for identifying such anomalies in theoretical models.

Looking ahead, our work points towards several promising avenues for future research:

1. In the literature (see references cited in section I), braiding phases, fusion coefficients, shrinking coefficients, and quantum dimensions have been determined for a concrete topological order. It is also important to practically determine the unitary matrices (i.e., F -, Δ -, and Δ^2 -symbols) introduced in this paper by solving pentagon equations and (hierarchical) shrinking-fusion hexagon equations. Solving these equations in the present work is expected to be very tedious (practical calculations in 3D can be found in references such as ref. [80]). While it is beyond the scope of the current paper, solving these equations undoubtedly represents a key step toward a more complete description of higher-dimensional topological orders. Recently, Quantinuum's H2 trapped-ion quantum processor [81] successfully realized a non-Abelian topological order in 3D spacetime and demonstrated control of its anyons. This topological order can be formally regarded as the lower-dimensional counterpart of the Borromean rings topological order proposed in ref. [38]. Efforts toward the experimental realization of 4D topological orders and control of loop excitations through the platform of trapped-ion quantum processors will provide experimental evidence for theoretical predic-

tions of the topological data of loop-like topological excitations.

2. In this paper, we solely focus on diagrams pertaining to fusion and shrinking rules, although it is worth noting that braiding statistics also hold significance in comprehending higher-dimensional topological orders. More concretely, we have defined F -, Δ -, and Δ^2 -symbols to perform unitary transformations associated with fusion and shrinking processes; however, we have not studied yet the higher-dimensional spacetime counterpart of R -symbol in 3D. While diagrammatic representation of braiding processes is definitely intricate due to the involvement of spatially extended excitations, incorporating braiding processes into our diagrammatic representations presents an intriguing avenue for future exploration. Doing so may unveil new diagrammatic rules capable of encoding more complete algebraic structures relevant to braiding, fusion, and shrinking processes. Based on all data depicted by field theory and consistency conditions in diagrammatic representations, it is further interesting to study the connection between our field-theory-inspired diagrammatic representations and categorical approach in the future.
3. BF theory exhibits a close relationship with non-invertible symmetry and symmetry topological field theory (SymTFT). Various twisted terms, along with their fusion rules and braiding statistics, have been involved in the context of SymTFT, including notable examples such as BB , BBA , and $AdAdA$ twisted terms, see, e.g., refs. [49, 51, 53, 55]. These topological terms were previously a focus of investigation in the field-theoretical description of higher-dimensional topological orders [29, 35, 70, 79]. It would be intriguing to explore the incorporation of shrinking and hierarchical shrinking rules [28, 29] into SymTFT and establish connections between SymTFT and our diagrammatic representations. Such investigations hold the potential to enrich our understanding of both SymTFT and the broader landscape of topological field theories.
4. In this paper, our focus is primarily on the diagrammatic representations of 4D and 5D topological orders. However, it is worth noting that the framework we have developed lends itself to potential generalization for arbitrarily higher-dimensional topological orders. Such generalization holds promise for providing deeper insights into the underlying structure and properties of higher-dimensional topological orders, warranting further exploration in future studies.

ACKNOWLEDGMENTS

P.Y. thanks Z.-C. Gu for the warm hospitality during the visit to the Chinese University of Hong Kong, where part of this work was conducted. This work was partially supported by the National Natural Science Foundation of China (NSFC) under Grant Nos. 12474149 and 12074438. The calculations reported were performed on resources provided by the Guangdong Provincial Key Laboratory of Magnetoelectric Physics and Devices (No. 2022B1212010008).

Appendix A: Review of anyon diagrams

In this appendix, we will briefly review the basic concepts in the diagrammatic representations of anyons. The diagrammatic rules and algebra set up the structure of anyon theories and they are closely related to TQFT descriptions.

1. Fusion rules and diagrammatic representations

Since shrinking rules are trivial in 3D, we do not need to put excitations in different sets and treat them differently. Consequently, we can easily recover the diagrammatic representations for anyons by drawing all fusion diagrams in a single-line fashion.

Suppose the anyonic fusion process $a \otimes b$ has fusion channels to c , we can represent this fusion process diagrammatically in figure 20. $\mu = \{1, 2, \dots, N_c^{ab}\}$ labels different fusion channels to c . The diagram can be defined as a vector $|a, b; c, \mu\rangle$, where different μ represent orthogonal vectors in the fusion space V_c^{ab} with $\dim(V_c^{ab}) = N_c^{ab}$. For fusing three anyons, suppose $(a \otimes b) \otimes c$ has fusion channels to d . Diagrammatically, we depict the process as the upper diagram shown in figure 21. Associativity indicates that the upper and the lower diagrams in figure 21 represent different bases and we can use the unitary F -symbol to change the basis. The definition of the F -symbol is given by figure 22.

For the diagrams involving four anyons, as shown in figure 23, we use the F -symbols to transform diagrams and derive the pentagon equation:

$$\sum_{\sigma=1}^{N_e^{fh}} [F_e^{fcd}]_{g\nu\lambda, h\gamma\sigma} [F_e^{abh}]_{f\mu\sigma, i\rho\delta} = \sum_j \sum_{\omega=1}^{N_g^{aj}} \sum_{\theta=1}^{N_j^{bc}} \sum_{\tau=1}^{N_i^d} [F_g^{abc}]_{f\mu\nu, j\theta\omega} [F_e^{ajd}]_{g\omega\lambda, i\tau\delta} [F_i^{bcd}]_{j\theta\tau, h\gamma\rho}. \quad (\text{A1})$$

No more identities beyond the pentagon equation can be derived by drawing more complicated

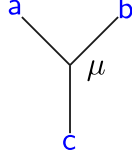


FIG. 20. Fusion diagram of two anyons. a , b and c denote anyons, $\mu = \{1, 2, \dots, N_c^{ab}\}$ labels different fusion channels to c .

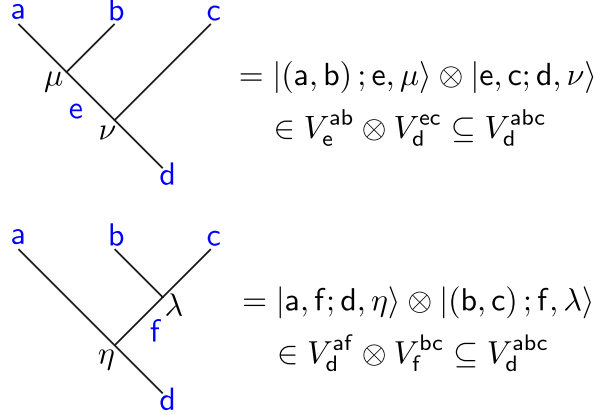


FIG. 21. Fusion diagram of three anyons. a , b , and c are input anyons and they finally fuse to d . The anyons in the bracket fuse together first. \otimes mean tensor product here. In the upper diagram, the set $\{|(a, b); e, \mu\rangle \otimes |e, c; d, \nu\rangle\}$ spans the whole space V_d^{abc} , where different μ , ν and e label different orthogonal vectors. Such space V_d^{abc} is isomorphic to $\oplus_e V_e^{ab} \otimes V_d^{ec}$ and thus $\dim(V_d^{abc}) = \sum_e N_e^{ab} N_d^{ec}$. For the lower diagram, the case is similar and we have $V_d^{abc} \cong \oplus_f V_d^{af} \otimes V_f^{bc}$, which indicates $\dim(V_d^{abc}) = \sum_f N_d^{af} N_f^{bc} = \sum_e N_e^{ab} N_d^{ec}$.

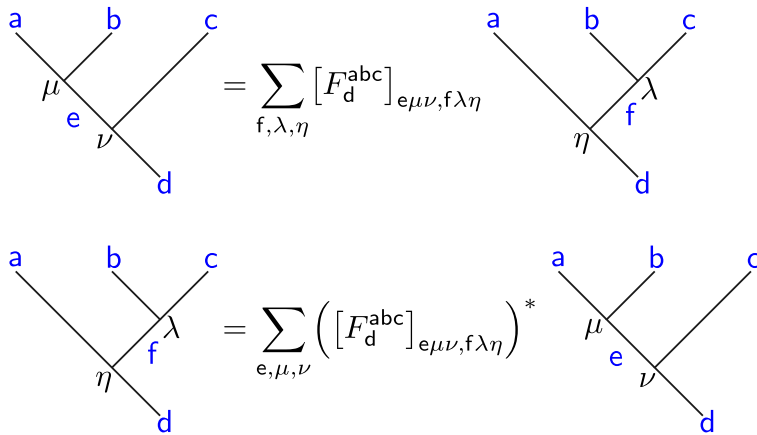


FIG. 22. Definition of F -symbol. The left and right diagrams describe the same physics in different bases. We use the unitary F -symbol to change the basis.

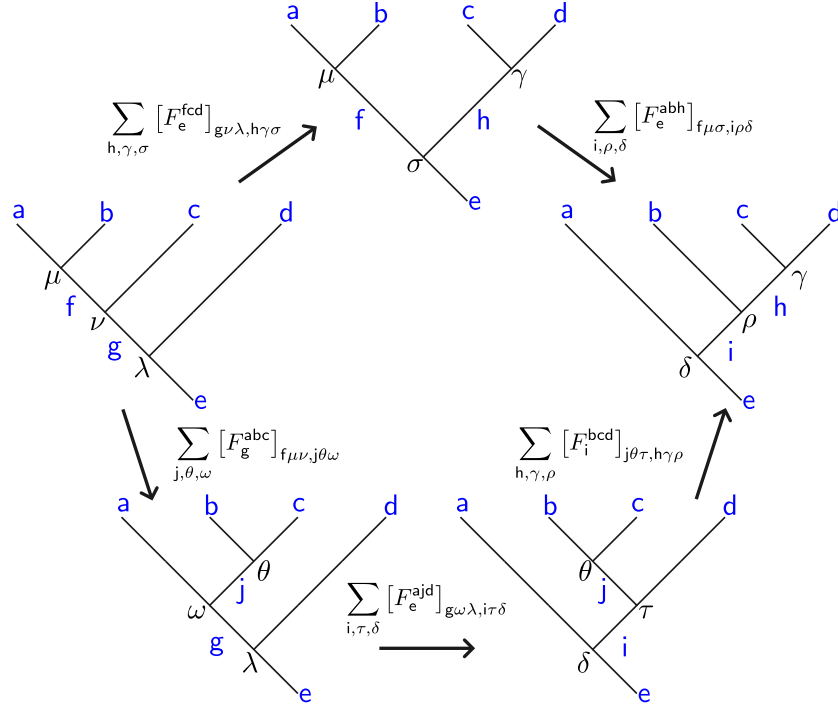


FIG. 23. Pentagon equation. We highlight anyons in blue. Starting from the far left diagram, we can go to the far right diagram through either the upper path or the lower path. Comparing these two different paths, we can derive the pentagon equation.

$$\begin{aligned}
 & \begin{array}{c} b \quad a \\ \diagdown \quad / \\ \mu \\ \diagup \quad \diagdown \\ c \end{array} = \sum_{\nu} [R_c^{ab}]_{\mu, \nu} \begin{array}{c} b \quad a \\ \diagdown \quad / \\ \nu \\ \diagup \quad \diagdown \\ c \end{array} \\
 & \begin{array}{c} b \quad a \\ \diagdown \quad / \\ \mu \\ \diagup \quad \diagdown \\ c \end{array} = \sum_{\nu} \left([R_c^{ba}]^{-1} \right)_{\mu, \nu} \begin{array}{c} b \quad a \\ \diagdown \quad / \\ \nu \\ \diagup \quad \diagdown \\ c \end{array}
 \end{aligned}$$

FIG. 24. Definition of R -symbol. The upper and lower diagrams correspond to over-crossing and under-crossing respectively. -1 denotes the inverse matrix. Since the R -symbol is unitary, $\left([R_c^{ba}]^{-1} \right)_{\mu, \nu}$ can be written as $\left([R_c^{ba}]_{\nu, \mu} \right)^*$.

fusion diagrams. A set of unitary F -symbols satisfying the pentagon equation form a unitary fusion category.

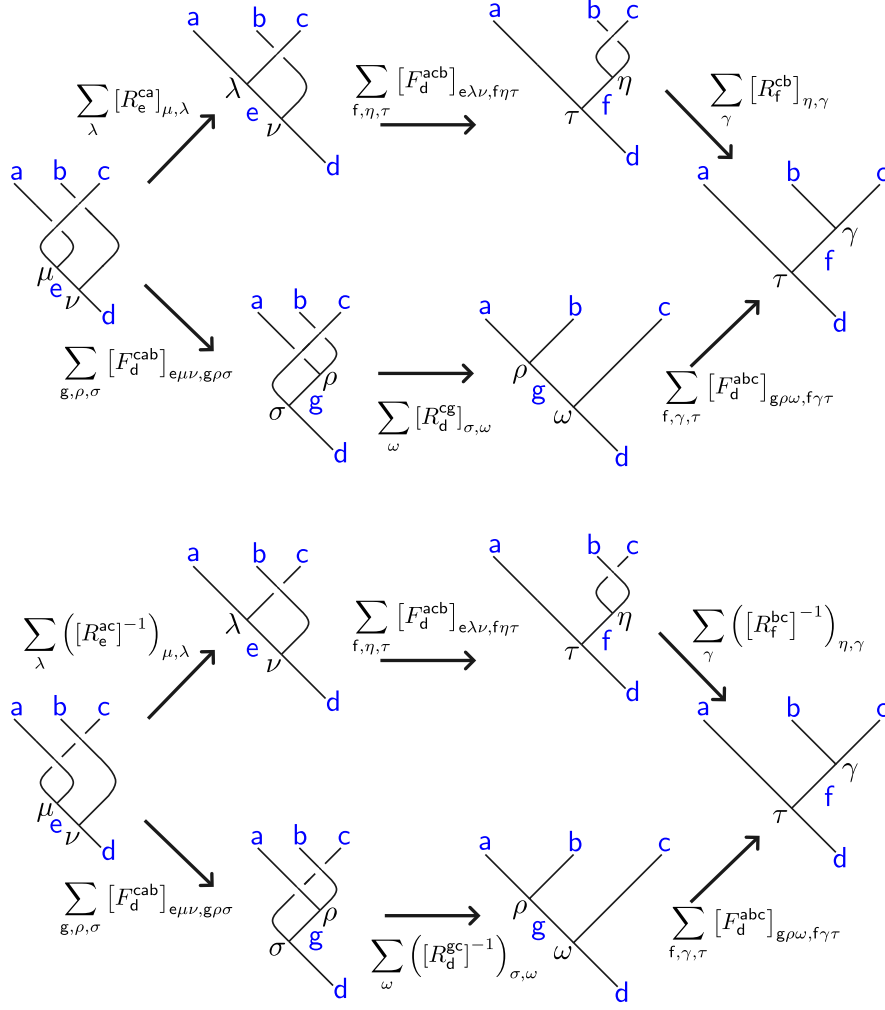


FIG. 25. Hexagon equations. We highlight anyons in blue. Eq. (A3) and eq. (A4) correspond to the upper (over-crossing) and the lower (under-crossing) hexagon diagrams. Similar to figure 23, for each hexagon diagram, we have two paths to transform the far left to the far right. Comparing the upper and the lower paths directly leads to eq. (A3) and eq. (A4).

2. Braiding statistics and diagrammatic representations

In section A 1, we only consider fusion processes, thus worldlines will not cross each other. In this section, we allow worldlines to cross over and under each other to form braiding processes. For Abelian anyons, a braiding process only accumulates a phase $e^{i\theta}$, which can be regarded as a one-dimensional representation of the braid group. However, for non-Abelian anyons, a braiding process is equivalent to multiplying a unitary matrix to the initial wavefunction of the system. This unitary matrix can be regarded as a higher-dimensional representation of the braid group.

Suppose a and b fuse to c. This process can be viewed as a vector in the fusion space V_c^{ab} . Due to the principle of locality, if we (half) braid a and b first and then fuse them together, the fusion output remains c. Consequently, this whole process can also be viewed as a vector in the space V_c^{ab} . These two vectors are related to each other through the R -symbol, as shown in figure 24. The upper and lower diagrams in figure 24 correspond to over-crossing and under-crossing respectively. $[R_c^{ba}]^{-1}$ is the inverse of $[R_c^{ba}]$. Similar to the F -symbol, the R -symbol is also unitary:

$$\sum_{\nu} [R_c^{ab}]_{\mu,\nu} \left([R_c^{ab}]_{\mu',\nu} \right)^* = \delta_{\mu\mu'}. \quad (\text{A2})$$

Consider using the F -symbols and R -symbols in the diagrams involving three anyons, as shown in figure 25, we can derive consistency relations for the F -symbols and R -symbols in 3D topological order, known as the hexagon equations:

$$\begin{aligned} & \sum_{\lambda=1}^{N_e^{ac}} \sum_{\eta=1}^{N_f^{cb}} [R_e^{ca}]_{\mu,\lambda} [F_d^{acb}]_{e\lambda\nu,f\eta\tau} [R_f^{cb}]_{\eta,\gamma} \\ &= \sum_g \sum_{\rho=1}^{N_g^{ab}} \sum_{\sigma=1}^{N_d^{cg}} \sum_{\omega=1}^{N_d^{gc}} [F_d^{cab}]_{e\mu\nu,g\rho\sigma} [R_d^{cg}]_{\sigma,\omega} [F_d^{abc}]_{g\rho\omega,f\gamma\tau}, \end{aligned} \quad (\text{A3})$$

$$\begin{aligned} & \sum_{\lambda=1}^{N_e^{ac}} \sum_{\eta=1}^{N_f^{cb}} \left([R_e^{ac}]^{-1} \right)_{\mu,\lambda} [F_d^{acb}]_{e\lambda\nu,f\eta\tau} \left([R_f^{bc}]^{-1} \right)_{\eta,\gamma} \\ &= \sum_g \sum_{\rho=1}^{N_g^{ab}} \sum_{\sigma=1}^{N_d^{cg}} \sum_{\omega=1}^{N_d^{gc}} [F_d^{cab}]_{e\mu\nu,g\rho\sigma} \left([R_d^{gc}]^{-1} \right)_{\sigma,\omega} [F_d^{abc}]_{g\rho\omega,f\gamma\tau}. \end{aligned} \quad (\text{A4})$$

Eq. (A3) and eq. (A4) correspond to the upper and the lower diagrams in figure 25 respectively. A set of unitary F -symbols and unitary R -symbols satisfying the pentagon and hexagon equations form a unitary braided tensor category. All 3D anyon theories must be in this form. Given all fusion rules, there are only finite gauge inequivalent solutions of the pentagon and hexagon equations.

Appendix B: Diagrams involving four excitations

In this appendix, we consider diagrams that involve four excitations and show that we cannot obtain new consistency relations besides the pentagon and shrinking-fusion hexagon equations from these diagrams.

Starting with $[[\mathcal{S}(a) \otimes \mathcal{S}(b)] \otimes \mathcal{S}(c)] \otimes \mathcal{S}(d)$, we can finally generate a total of 21 distinct diagrams by utilizing the F - and Δ -symbols. We list all these diagrams in figure 26 and omit all

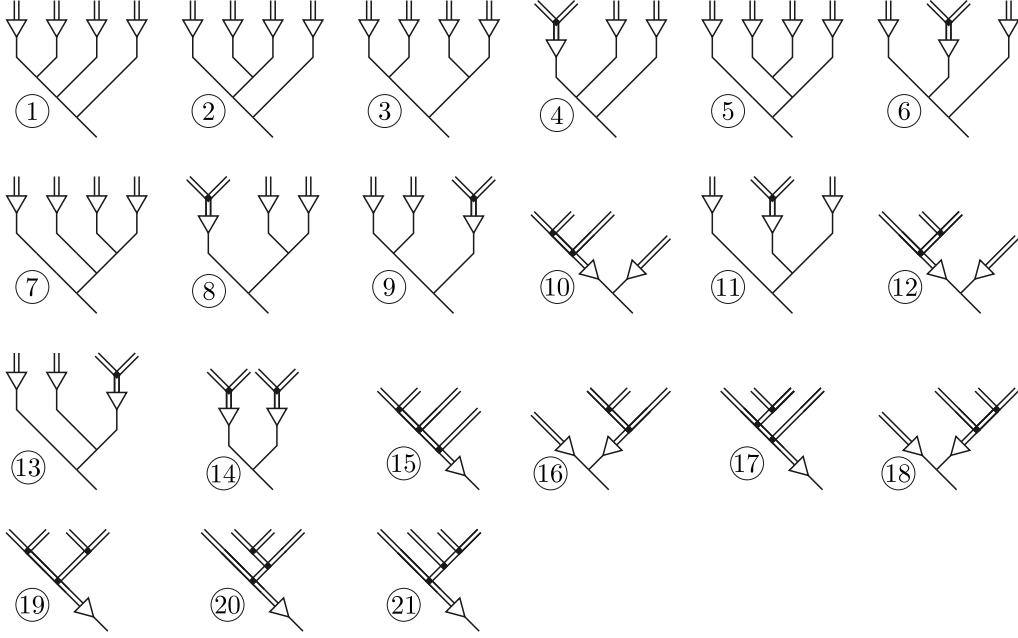


FIG. 26. All 21 diagrams that involve four topological excitations. We label them from 1 to 21 and their relations are given in figure 27.

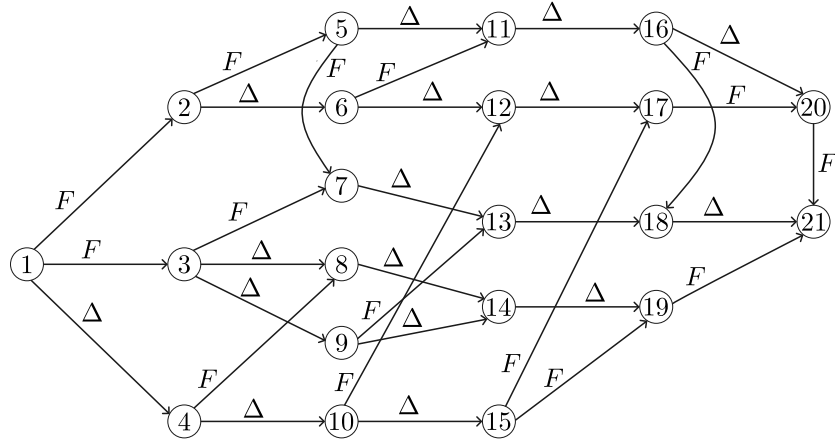


FIG. 27. The relations between the 21 diagrams. An arrow with F or Δ means that we can use F - or Δ -symbols to transform the diagram. For example, diagram 1 can be transformed to diagram 3 by using an F -symbol, diagram 3 can be transformed to diagram 9 by using a Δ -symbol.

excitation and channel labels for simplicity. The relations between these 21 diagrams are shown in figure 27, where we use arrows with F or Δ to indicate transformations via the F - or Δ -symbols. From figure 27 we can find 13 candidates for independent polygon equations as shown in figure 28. However, upon recovering the excitation and channel labels and attempting to write down the

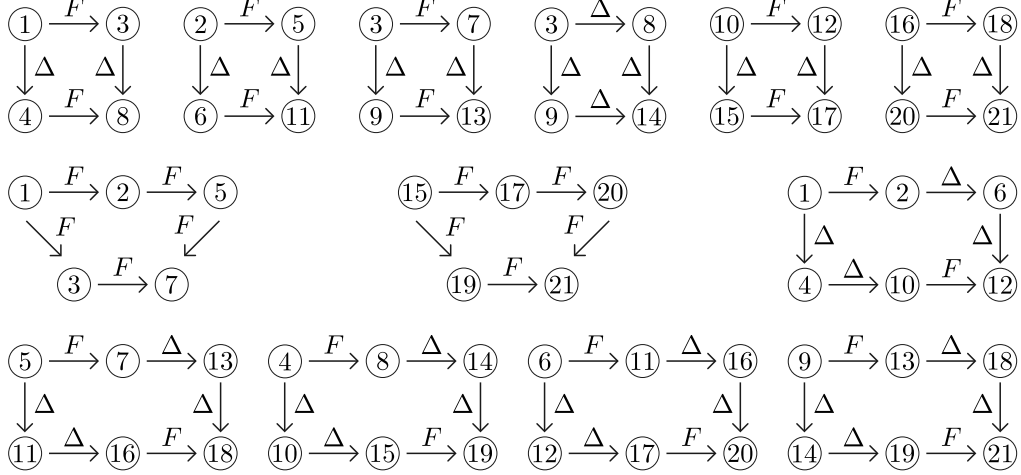


FIG. 28. 13 polygons from figure 27. It turns out that all quadrilateral equations are trivial. Pentagons and hexagons essentially give the independent pentagon and shrinking-fusion hexagon equations.

consistent equations, we find that only the pentagon and shrinking-fusion hexagon equations are independent, while the other equations are automatically satisfied and thus trivial.

To be more specific, we consider the quadrilateral equation given by diagrams 1, 3, 4, and 8 as an example. The transformations $1 \rightarrow 3 \rightarrow 8$ and $1 \rightarrow 3 \rightarrow 4$ give coefficients

$$1 \rightarrow 3 \rightarrow 8 : \sum_{m,\gamma,\eta} \sum_{n,\delta,\tau} [F_k^{\text{igh}}]_{j\sigma\lambda,m\gamma\eta} [\Delta_i^{\text{ab}}]_{ef\mu\nu\rho,n\delta\tau}$$

$$1 \rightarrow 4 \rightarrow 8 : \sum_{n,\delta,\tau} \sum_{m,\gamma,\eta} [\Delta_i^{\text{ab}}]_{ef\mu\nu\rho,n\delta\tau} [F_k^{\text{igh}}]_{j\sigma\lambda,m\gamma\eta}$$

respectively. We can see that they equal to each other automatically and thus the quadrilateral equation is trivial. For a similar reason, other quadrilateral equations are also trivial. The two pentagons in figure 28 respectively give the pentagon equations for $\{a, b, c, d\}$ and $\{\mathcal{S}(a), \mathcal{S}(b), \mathcal{S}(c), \mathcal{S}(d)\}$, where $a, b, c, d \in \Phi_0^4$. Since $\mathcal{S}(a), \mathcal{S}(b), \mathcal{S}(c), \mathcal{S}(d) \in \Phi_1^4 \subseteq \Phi_0^4$, the later pentagon equation is automatically satisfied when we demand that the former pentagon equation holds. The five hexagons shown in figure 28 give the shrinking-fusion hexagon equations for $\{a, b, c\}$, $\{b, c, d\}$, $\{(a \otimes b), c, d\}$, $\{a, (b \otimes c), d\}$ and $\{a, b, (c \otimes d)\}$ respectively and essentially they are the same equation. Thus we conclude that there are only two independent equations

in figure 28, which are the pentagon and shrinking-fusion hexagon equations.

- [1] B. Zeng, X. Chen, D.-L. Zhou, and X.-G. Wen, Quantum information meets quantum matter – from quantum entanglement to topological phase in many-body systems (2018), [arXiv:1508.02595 \[cond-mat.str-el\]](#).
- [2] X.-G. Wen, Colloquium: Zoo of quantum-topological phases of matter, [Rev. Mod. Phys. 89, 041004 \(2017\)](#).
- [3] E. Witten, Quantum field theory and the jones polynomial, [Commun. Math. Phys. 121, 351 \(1989\)](#).
- [4] V. G. Turaev, [Quantum Invariants of Knots and 3-Manifolds](#) (De Gruyter, Berlin, Boston, 2016).
- [5] B. Blok and X. G. Wen, Effective theories of the fractional quantum hall effect at generic filling fractions, [Phys. Rev. B 42, 8133 \(1990\)](#).
- [6] C. Nayak", Non-abelian anyons and topological quantum computation, [Reviews of Modern Physics 80, 1083 \(2008\)](#).
- [7] X.-G. Wen, [Quantum field theory of many-body systems: from the origin of sound to an origin of light and electrons](#) (Oxford University Press, 2004).
- [8] Y.-M. Lu and A. Vishwanath, Theory and classification of interacting integer topological phases in two dimensions: A chern-simons approach, [Phys. Rev. B 86, 125119 \(2012\)](#).
- [9] P. Ye and X.-G. Wen, Projective construction of two-dimensional symmetry-protected topological phases with $u(1)$, $so(3)$, or $su(2)$ symmetries, [Phys. Rev. B 87, 195128 \(2013\)](#).
- [10] Z.-C. Gu, J. C. Wang, and X.-G. Wen, Multikink topological terms and charge-binding domain-wall condensation induced symmetry-protected topological states: Beyond chern-simons/bf field theories, [Phys. Rev. B 93, 115136 \(2016\)](#).
- [11] L.-Y. Hung and Y. Wan, k matrix construction of symmetry-enriched phases of matter, [Phys. Rev. B 87, 195103 \(2013\)](#).
- [12] A. Kitaev, Anyons in an exactly solved model and beyond, [Annals of Physics 321, 2 \(2006\)](#), january Special Issue.
- [13] M. A. Levin and X.-G. Wen, String-net condensation: A physical mechanism for topological phases, [Phys. Rev. B 71, 045110 \(2005\)](#).
- [14] X. Chen, Z.-C. Gu, and X.-G. Wen, Local unitary transformation, long-range quantum entanglement, wave function renormalization, and topological order, [Phys. Rev. B 82, 155138 \(2010\)](#).

- [15] P. H. Bonderson, *Non-Abelian Anyons and Interferometry*, **Ph.D. thesis**, California Institute of Technology. (2007).
- [16] E. Ardonne and J. Slingerland, Clebsch-gordan and 6j-coefficients for rank 2 quantum groups, **Journal of Physics A: Mathematical and Theoretical** **43**, 395205 (2010).
- [17] P. Bonderson, K. Shtengel, and J. Slingerland, Interferometry of non-abelian anyons, **Annals of Physics** **323**, 2709 (2008).
- [18] I. S. Eliëns, J. C. Romers, and F. A. Bais, Diagrammatics for bose condensation in anyon theories, **Phys. Rev. B** **90**, 195130 (2014).
- [19] S. H. Simon, *Topological quantum* (Oxford University Press, 2023).
- [20] L. Kong and X.-G. Wen, Braided fusion categories, gravitational anomalies, and the mathematical framework for topological orders in any dimensions (2014), [arXiv:1405.5858 \[cond-mat.str-el\]](https://arxiv.org/abs/1405.5858).
- [21] M. Barkeshli, P. Bonderson, M. Cheng, and Z. Wang, Symmetry fractionalization, defects, and gauging of topological phases, **Phys. Rev. B** **100**, 115147 (2019).
- [22] J. M. Leinaas and J. Myrheim, On the theory of identical particles, **Il Nuovo Cimento B (1971-1996)** **37**, 1 (1977).
- [23] Y.-S. Wu, General theory for quantum statistics in two dimensions, **Phys. Rev. Lett.** **52**, 2103 (1984).
- [24] M. G. Alford and F. Wilczek, Aharonov-bohm interaction of cosmic strings with matter, **Phys. Rev. Lett.** **62**, 1071 (1989).
- [25] L. M. Krauss and F. Wilczek, Discrete gauge symmetry in continuum theories, **Phys. Rev. Lett.** **62**, 1221 (1989).
- [26] F. Wilczek and A. Zee, Linking numbers, spin, and statistics of solitons, **Phys. Rev. Lett.** **51**, 2250 (1983).
- [27] A. S. Goldhaber, R. MacKenzie, and F. Wilczek, Field corrections to induced statistics, **Mod. Phys. Lett. A** **4**, 21 (1989).
- [28] Z.-F. Zhang, Q.-R. Wang, and P. Ye, Non-abelian fusion, shrinking, and quantum dimensions of abelian gauge fluxes, **Phys. Rev. B** **107**, 165117 (2023).
- [29] Y. Huang, Z.-F. Zhang, and P. Ye, Fusion rules and shrinking rules of topological orders in five dimensions, **JHEP** **11**, 210, [arXiv:2306.14611 \[hep-th\]](https://arxiv.org/abs/2306.14611).
- [30] G. T. Horowitz and M. Srednicki, A quantum field theoretic description of linking numbers and their generalization, **Commun.Math. Phys.** **130**, 83 (1990).
- [31] P. Ye, T. L. Hughes, J. Maciejko, and E. Fradkin, Composite particle theory of three-dimensional

- gapped fermionic phases: Fractional topological insulators and charge-loop excitation symmetry, *Phys. Rev. B* **94**, 115104 (2016).
- [32] B. Moy, H. Goldman, R. Sohal, and E. Fradkin, Theory of oblique topological insulators, *SciPost Phys.* **14**, 023 (2023).
- [33] P. Ye and X.-G. Wen, Constructing symmetric topological phases of bosons in three dimensions via fermionic projective construction and dyon condensation, *Phys. Rev. B* **89**, 045127 (2014).
- [34] P. Putrov, J. Wang, and S.-T. Yau, Braiding statistics and link invariants of bosonic/fermionic topological quantum matter in 2+1 and 3+1 dimensions, *Annals of Physics* **384**, 254 (2017).
- [35] Q.-R. Wang, M. Cheng, C. Wang, and Z.-C. Gu, Topological quantum field theory for abelian topological phases and loop braiding statistics in $(3 + 1)$ -dimensions, *Phys. Rev. B* **99**, 235137 (2019).
- [36] P. Ye and Z.-C. Gu, Topological quantum field theory of three-dimensional bosonic abelian-symmetry-protected topological phases, *Phys. Rev. B* **93**, 205157 (2016).
- [37] X. Wen, H. He, A. Tiwari, Y. Zheng, and P. Ye, Entanglement entropy for $(3+1)$ -dimensional topological order with excitations, *Phys. Rev. B* **97**, 085147 (2018).
- [38] A. P. O. Chan, P. Ye, and S. Ryu, Braiding with borromean rings in $(3 + 1)$ -dimensional spacetime, *Phys. Rev. Lett.* **121**, 061601 (2018).
- [39] Z.-F. Zhang and P. Ye, Compatible braidings with Hopf links, multi-loop, and Borromean rings in $(3+1)$ -dimensional spacetime, *Phys. Rev. Research* **3**, 023132 (2021).
- [40] P. Ye and Z.-C. Gu, Vortex-line condensation in three dimensions: A physical mechanism for bosonic topological insulators, *Phys. Rev. X* **5**, 021029 (2015).
- [41] P. Ye and J. Wang, Symmetry-protected topological phases with charge and spin symmetries: Response theory and dynamical gauge theory in two and three dimensions, *Phys. Rev. B* **88**, 235109 (2013).
- [42] S. Schafer-Nameki, Ictp lectures on (non-)invertible generalized symmetries (2023), [arXiv:2305.18296 \[hep-th\]](https://arxiv.org/abs/2305.18296).
- [43] B. Heidenreich, J. McNamara, M. Montero, M. Reece, T. Rudelius, and I. Valenzuela, Non-invertible global symmetries and completeness of the spectrum, *Journal of High Energy Physics* **2021**, 203 (2021), [arXiv:2104.07036 \[hep-th\]](https://arxiv.org/abs/2104.07036).
- [44] J. Kaidi, K. Ohmori, and Y. Zheng, Kramers-wannier-like duality defects in $(3 + 1)d$ gauge theories, *Phys. Rev. Lett.* **128**, 111601 (2022).
- [45] Y. Choi, C. Córdova, P.-S. Hsin, H. T. Lam, and S.-H. Shao, Noninvertible duality defects in $3 + 1$

- dimensions, *Phys. Rev. D* **105**, 125016 (2022).
- [46] K. Roumpedakis, S. Seifnashri, and S.-H. Shao, Higher Gauging and Non-invertible Condensation Defects, *Communications in Mathematical Physics* **401**, 3043 (2023), [arXiv:2204.02407 \[hep-th\]](#).
- [47] J. Kaidi, G. Zafrir, and Y. Zheng, Non-invertible symmetries of $N = 4$ SYM and twisted compactification, *Journal of High Energy Physics* **2022**, 53 (2022), [arXiv:2205.01104 \[hep-th\]](#).
- [48] J. Kaidi, K. Ohmori, and Y. Zheng, Symmetry TFTs for Non-invertible Defects, *Communications in Mathematical Physics* **404**, 1021 (2023), [arXiv:2209.11062 \[hep-th\]](#).
- [49] J. Kaidi, E. Nardoni, G. Zafrir, and Y. Zheng, Symmetry TFTs and anomalies of non-invertible symmetries, *Journal of High Energy Physics* **2023**, 53 (2023), [arXiv:2301.07112 \[hep-th\]](#).
- [50] Y. Choi, C. Córdova, P.-S. Hsin, H. T. Lam, and S.-H. Shao, Non-invertible Condensation, Duality, and Triality Defects in 3+1 Dimensions, *Communications in Mathematical Physics* **402**, 489 (2023), [arXiv:2204.09025 \[hep-th\]](#).
- [51] A. Antinucci and F. Benini, Anomalies and gauging of $u(1)$ symmetries (2024), [arXiv:2401.10165 \[hep-th\]](#).
- [52] J. A. Damia, R. Argurio, and E. Garcia-Valdecasas, Non-invertible defects in 5d, boundaries and holography, *SciPost Phys.* **14**, 067 (2023).
- [53] Riccardo Argurio, Francesco Benini, Matteo Bertolini, Giovanni Galati, and Pierluigi Niro, On the symmetry tft of yang-mills-chern-simons theory, *Journal of High Energy Physics* **2024**, 130 (2024), [arXiv:arXiv:2404.06601 \[hep-th\]](#).
- [54] W. Cao and Q. Jia, Symmetry tft for subsystem symmetry (2024), [arXiv:2310.01474 \[hep-th\]](#).
- [55] T. D. Brennan and Z. Sun, A symtft for continuous symmetries (2024), [arXiv:2401.06128 \[hep-th\]](#).
- [56] T. Hansson, V. Oganessian, and S. Sondhi, Superconductors are topologically ordered, *Annals of Physics* **313**, 497 (2004).
- [57] J. Preskill and L. M. Krauss, Local discrete symmetry and quantum-mechanical hair, *Nuclear Physics B* **341**, 50 (1990).
- [58] M. G. Alford, K.-M. Lee, J. March-Russell, and J. Preskill, Quantum field theory of non-abelian strings and vortices, *Nuclear Physics B* **384**, 251 (1992).
- [59] C. Wang and M. Levin, Braiding statistics of loop excitations in three dimensions, *Phys. Rev. Lett.* **113**, 080403 (2014).
- [60] J. C. Wang, Z.-C. Gu, and X.-G. Wen, Field-theory representation of gauge-gravity symmetry-protected topological invariants, group cohomology, and beyond, *Phys. Rev. Lett.* **114**, 031601 (2015).

- [61] J. C. Wang and X.-G. Wen, Non-abelian string and particle braiding in topological order: Modular $SL(3, \mathbb{Z})$ representation and $(3 + 1)$ -dimensional twisted gauge theory, *Phys. Rev. B* **91**, 035134 (2015).
- [62] C.-M. Jian and X.-L. Qi, Layer construction of 3d topological states and string braiding statistics, *Phys. Rev. X* **4**, 041043 (2014).
- [63] S. Jiang, A. Mesaros, and Y. Ran, Generalized modular transformations in $(3 + 1)$ D topologically ordered phases and triple linking invariant of loop braiding, *Phys. Rev. X* **4**, 031048 (2014).
- [64] C. Wang, C.-H. Lin, and M. Levin, Bulk-boundary correspondence for three-dimensional symmetry-protected topological phases, *Phys. Rev. X* **6**, 021015 (2016).
- [65] A. Tiwari, X. Chen, and S. Ryu, Wilson operator algebras and ground states of coupled BF theories, *Phys. Rev. B* **95**, 245124 (2017).
- [66] A. Kapustin and R. Thorngren, Anomalies of discrete symmetries in various dimensions and group cohomology, ArXiv e-prints (2014), [arXiv:1404.3230 \[hep-th\]](https://arxiv.org/abs/1404.3230).
- [67] Y. Wan, J. C. Wang, and H. He, Twisted gauge theory model of topological phases in three dimensions, *Phys. Rev. B* **92**, 045101 (2015).
- [68] X. Chen, A. Tiwari, and S. Ryu, Bulk-boundary correspondence in $(3+1)$ -dimensional topological phases, *Phys. Rev. B* **94**, 045113 (2016).
- [69] A. Kapustin and N. Seiberg, Coupling a QFT to a TQFT and Duality, *JHEP* **04**, 001, [arXiv:1401.0740 \[hep-th\]](https://arxiv.org/abs/1401.0740).
- [70] Z.-F. Zhang, Q.-R. Wang, and P. Ye, Continuum field theory of three-dimensional topological orders with emergent fermions and braiding statistics, *Phys. Rev. Res.* **5**, 043111 (2023).
- [71] X.-L. Qi and S.-C. Zhang, Topological insulators and superconductors, *Rev. Mod. Phys.* **83**, 1057 (2011).
- [72] M. F. Lapa, C.-M. Jian, P. Ye, and T. L. Hughes, Topological electromagnetic responses of bosonic quantum hall, topological insulator, and chiral semimetal phases in all dimensions, *Phys. Rev. B* **95**, 035149 (2017).
- [73] P. Ye, M. Cheng, and E. Fradkin, Fractional s -duality, classification of fractional topological insulators, and surface topological order, *Phys. Rev. B* **96**, 085125 (2017).
- [74] E. Witten, Fermion path integrals and topological phases, *Rev. Mod. Phys.* **88**, 035001 (2016).
- [75] B. Han, H. Wang, and P. Ye, Generalized wen-zee terms, *Phys. Rev. B* **99**, 205120 (2019).
- [76] S.-Q. Ning, Z.-X. Liu, and P. Ye, Fractionalizing global symmetry on looplike topological excitations,

- Phys. Rev. B* **105**, 205137 (2022).
- [77] S.-Q. Ning, Z.-X. Liu, and P. Ye, Symmetry enrichment in three-dimensional topological phases, *Phys. Rev. B* **94**, 245120 (2016).
- [78] P. Ye, Three-dimensional anomalous twisted gauge theories with global symmetry: Implications for quantum spin liquids, *Phys. Rev. B* **97**, 125127 (2018).
- [79] Z.-F. Zhang and P. Ye, Topological orders, braiding statistics, and mixture of two types of twisted BF theories in five dimensions, *J. High Energ. Phys.* **2022** (4), 138.
- [80] X. G. Wen, *A theory of 2+1D bosonic topological orders* (2016), [arXiv:1506.05768](https://arxiv.org/abs/1506.05768).
- [81] M. Iqbal, N. Tantivasadakarn, R. Verresen, S. L. Campbell, J. M. Dreiling, C. Figgatt, J. P. Gaebler, J. Johansen, M. Mills, S. A. Moses, J. M. Pino, A. Ransford, M. Rowe, P. Siegfried, R. P. Stutz, M. Foss-Feig, A. Vishwanath, and H. Dreyer, Non-Abelian topological order and anyons on a trapped-ion processor, *Nature (London)* **626**, 505 (2024), [arXiv:2305.03766](https://arxiv.org/abs/2305.03766) [quant-ph].